Geoscience Frontiers 15 (2024) 101774

Contents lists available at ScienceDirect

Geoscience Frontiers

journal homepage: www.elsevier.com/locate/gsf

Research Paper

Impacts and risks of "realistic" global warming projections for the 21st century

Nicola Scafetta

Department of Earth Sciences, Environment and Georesources, University of Naples Federico II, Complesso Universitario di Monte S. Angelo, Via Vicinale Cupa Cintia, 21, 80126 Naples, NA, Italy

ARTICLE INFO

Article history:
Received 23 October 2023
Revised 8 December 2023
Accepted 16 December 2023
Available online 22 December 2023
Handling Editor: M. Santosh

Keywords:
Climate change
Climate models
Shared socioeconomic pathways
21st-century climate projections
Impacts and risks assessment

ABSTRACT

The IPCC AR6 assessment of the impacts and risks associated with projected climate changes for the 21st century is both alarming and ambiguous. According to computer projections, global surface temperature may warm from 1.3 °C to 8.0 °C by 2100, depending on the global climate model (GCM) and the shared socioeconomic pathway (SSP) scenario used for the simulations. Actual climate-change hazards are estimated to be high and very high if the global surface temperature rises, respectively, more than 2.0 °C and 3.0 °C above pre-industrial levels. Recent studies, however, showed that a substantial number of CMIP6 GCMs run "too hot" because they appear to be too sensitive to radiative forcing, and that the high/extreme emission scenarios SSP3-7.0 and SSP5-8.5 are to be rejected because judged to be unlikely and highly unlikely, respectively. Yet, the IPCC AR6 mostly focused on such alarmistic scenarios for risk assessments. This paper examines the impacts and risks of "realistic" climate change projections for the 21st century generated by assessing the theoretical models and integrating them with the existing empirical knowledge on global warming and the various natural cycles of climate change that have been recorded by a variety of scientists and historians. This is achieved by combining the SSP2-4.5 scenario (which is the most likely SSP according to the current policies reported by the International Energy Agency) and empirically optimized climate modeling. According to recent research, the GCM macro-ensemble that best hindcast the global surface warming observed from 1980 to 1990 to 2012–2022 should be made up of models that are characterized by a low equilibrium climate sensitivity (ECS) (1.5 °C < ECS ≤ 3.0 °C), in contrast to the IPCC AR6 likely and very likely ECS ranges at 2.5–4.0 °C and 2.0–5.0 °C, respectively. I show that the low-ECS macro-GCM with the SSP2-4.5 scenario projects a global surface temperature warming of 1.68–3.09 °C by 2080–2100 instead of 1.98–3.82 °C obtained with the GCMs with ECS in the 2.5–4.0 °C range. However, if the global surface temperature records are affected by significant non-climatic warm biases — as suggested by satellite-based lower troposphere temperature records and current studies on urban heat island effects — the same climate simulations should be scaled down by about 30%, resulting in a warming of about 1.18–2.16 °C by 2080–2100. Furthermore, similar moderate warming estimates (1.15–2.52 °C) are also projected by alternative empirically derived models that aim to recreate the decadal-to-millennial natural climatic oscillations, which the GCMs do not reproduce. The proposed methodologies aim to simulate hypothetical models supposed to optimally hindcast the actual available data. The obtained climate projections show that the expected global surface warming for the 21st-century will likely be mild, that is, no more than 2.5–3.0 °C and, on average, likely below the 2.0 °C threshold. This should allow for the mitigation and management of the most dangerous climate-change related hazards through appropriate low-cost adaptation policies. In conclusion, enforcing expensive decarbonization and net-zero emission scenarios, such as SSP1-2.6, is not required because the Paris Agreement temperature target of keeping global warming < 2 °C throughout the 21st century should be compatible also with moderate and pragmatic shared socioeconomic pathways such as the SSP2-4.5.

E-mail address: nicola.scafetta@unina.it

https://doi.org/10.1016/j.gsf.2023.101774
1674-9871/

1. Introduction

The IPCC Sixth Assessment Report (AR6) Working Group II (Pörtner et al., 2022) assessed that the environmental impacts of climate changes in the 21st century — such as rising sea levels and temperatures, increased extreme weather events, droughts and floods, and the spread of wildfires — could significantly affect environments, societies and many aspects of human economy and life. Projected climate changes could also directly and indirectly impact human health by inducing changes in many environmental factors associated with infectious and respiratory diseases, changes in heat and cold-related morbidity and mortality, changes in food production, changes in sociopolitical tensions and conflicts, and many others (Rocque et al., 2021).

In fact, despite CO_2 is, strictly speaking, not a pollutant, and its atmospheric increase is actually greening the Earth due to its fertilization effects (Zhu et al., 2016; Piao et al., 2019) and a warmer climate does also present a number of benefits, today there is growing concern that, during the 21st century, global warming induced by anthropogenic greenhouse gas emissions due to the persistent use of fossil fuels (which mostly emits CO_2) could exceed temperature levels that are considered sustainable with the current adaptive capacity of most communities (Masson-Delmotte et al., 2018, 2021). It is claimed that dangerous levels of global warming could be exceeded by as soon as 2050 unless a number of expensive adaptation and mitigation strategies are implemented such as energy policies attempting to reach net-zero emissions by about 2050 (Shukla et al., 2022; European Commission, 2023).

The term "net-zero emissions" refers to attaining a net balance between manmade greenhouse gas (GHG) emissions produced and GHG emissions removed from the atmosphere. Given the present limited possibility to remove GHGs from the atmosphere, net-zero requires swiftly limiting the use of fossil fuels – coal, oil, and gas – and transitioning toward renewable green-energy in all sectors of the economy.

Depending on the magnitude and speed of the evolving physical processes, climate changes may have both beneficial and harmful consequences. These effects are under the control of complex and still poorly understood nonlinear dynamical systems. As the temperature continues to warm, some nations may see immediate advantages, but the long-term consequences could be harmful, while others may see the opposite. Depending on elements including geographic location, socioeconomic conditions, and capacity for adaptation, the distribution of climate-change impacts and risks also considerably changes from place to place. By aggregating several indicators, Tol (2015) estimated that climate change could globally have a net positive economic welfare impact only if the global surface warming remains roughly < 2.0 °C above its 1850–1900 pre-industrial levels throughout the 21st century. However, Tol (2015) also highlighted the large uncertainty associated with such claims because, for example, on eleven analyzed economical risk estimates for a warming of 2.5 °C, it was found that the researchers disagree on the sign of the net impact: four were positive and seven negative.

For example, most of the early net gains should occur because increasing carbon dioxide in the atmosphere reduces water stress in plants, causing them to grow quicker, and because wealthy countries are mostly concentrated in temperate climatic zones, which should benefit more from a moderate warming. However, if the temperature rises too much, the water stress in the plants could grow. In general, although the situation varies from place to place, the scientific literature suggests that on a global scale, even if there may be initial economic net gains from global warming, such gains may be offset by losses as the environment continues to warm (particularly > 2.5–3.0 °C) in a too short time period (Pörtner et al., 2022). After then, societies will be able to recover economically only after effectively adapting to the new climatic conditions.

The Working Group I of the IPCC AR6 (Masson-Delmotte et al., 2021) stated that the global surface temperature in the first two decades of the 21st century (2001–2020) was about 1 °C (0.84–1.10 °C range) higher than the (1850–1900) pre-industrial period. Current computer-based global climate models (GCMs) suggest that the 1.5 °C warming level could, on average, be easily exceeded by as early as 2030, and the 2 °C warming level could be exceeded by about 2050–2060 (Masson-Delmotte et al., 2018, 2021). Consequently, because the global surface temperature is expected to rise very fast, climate changes are being considered by the United Nations a kind of imminent threat, especially for the impoverished societies that could lack the resources required for quickly cope and/or adapt to it. Thus, aggressive, and expensive climate policies aimed at significantly reducing anthropogenic greenhouse gas emissions from fossil fuels are being advocated for mitigating future climate changes in annual COPs (Conferences of the Parties) promoted by United Nations since 1995.

For example, in 2015 at COP-21 in Paris the UNFCCC (2023) reached a landmark agreement to combat climate change by promoting international policies to keep global warming "below 2 °C" (Gao et al., 2017) while even pursuing ambitious efforts "to limit the temperature increase to 1.5 °C above pre-industrial levels" by 2030 by enforcing Net-Zero by 2050 policies. Masson-Delmotte et al. (2018) and Meinshausen et al. (2022) argued that only by executing the Paris Agreement pledges of net-zero emissions by 2050 could restrict global surface warming to less than the "safe" threshold of about 2 °C. For similar reasons, editors of geoscience and health journals have being calling for urgent collective climate-mitigation actions (McNutt, 2015) because "our planet is in crisis" (Filippelli et al., 2021) and because the projected global warming for the 21st century would be the "greatest threat to global public health" (Atwoli et al., 2021) if not immediately mitigated as agreed in Paris. However, many severe uncertainties and concerns on such claims remain.

In fact, fossil fuels continue to supply most of the inexpensive energy that is today used worldwide, which is allowing developing countries to quickly raise their living and welfare standards. Indeed, while wealthy Western Nations seek to phase out coal power plants and, in general, are attempting to substantially limit the use of fossil fuels through impractical, expensive and unpopular rapid-decarbonization policies, the majority of the rest of the world is significantly increasing their emissions (Crippa et al., 2023). In particular, China, India, Indonesia, Japan and Vietnam, among other Asian countries, are constructing about 400 coal-fired power plants and planning to build another 400 units in the future years (GEM, 2023). Furthermore, the rapid depletion of critical metals required for a rapid shift from fossil fuel to renewable green-energies calls the possibility of such a technological transition into serious doubt (Groves et al., 2023) and, in general, economic meta-analyses indicate that the costs of implementing the net-zero policies required to meet the Paris climate targets may outweigh the benefits even in the worst-case-scenario global warming (Tol, 2023). As a result, there is no political agreement among world nations on how to manage future climate-change-related hazards.

World nations disagree on the actual threats, and, in fact, they prioritize different issues, likely because of the scientific uncertainty about future climate changes, as well as of their potential impacts and associated risks. The still existing large scientific uncertainty on this matter may lead to detrimental decisions either if a climatic alarm is overstated or understated. Policy disparities among countries would make finding effective solutions to potential climate-change-related hazards hard, while also risking harmful economic imbalances in the interactions between and within states. It should be evident to all that if a few wealthy countries significantly reduce their emissions while all the others significantly raise them, total emissions may not fall but, instead, increase and climate change will not be mitigated. For example, net-zero emission policies are being strongly advocated in the 27 nations of the European Union that, however, in 2022 contributed only 6.7% of the GHG global total emissions (Crippa et al., 2023); moreover, in the year 2022 several EU countries – including Italy (6.70 t CO_2eq/cap) and France (6.50 t CO_2eq/cap) – produced GHG per capita emissions less than the world global average (6.76 t CO_2eq/cap).

As a result, the range of potential impacts and risks related to projected climate changes for the 21st century must be restricted and estimated more precisely by constraining the various existing physical and economic uncertainties. This operation is necessary to conduct proper cost-benefit analyses of the required mitigation and/or adaptation policies in the hope that by being less controversial they could be more likely accepted by all nations. In fact, either underestimating or exaggerating the alarm of a possible climate-change crisis could have harmful economic implications that can negatively impact human economy and life at both global and local scales.

The main scientific uncertainties surrounding the physics of climate change are reviewed in Section 2, along with how they could be significantly constrained by using recent advances in scientific knowledge. Realistic projections of climate changes for the 21st century and their associated impacts and risks are evaluated in Section 4. Finally, Section 5 proposes an alternative interpretation based on empirical climate change modeling for the 21st-century that takes into account the implications of additional physical uncertainties concerning the temperature data and the actual warming, and the likely role of the Sun (Connolly et al., 2021; Scafetta, 2023c; Scafetta and Bianchini, 2023; Soon et al., 2023) and natural oscillations (Scafetta, 2013, 2021b) that are not properly modeled by the GCMs. This article only evaluates "realistic" climate change projections while assuming valid the economic and welfare models used by the IPCC (Shukla et al., 2022) to assess the impacts and risks that might be associated with projected levels of global warming.

2. Understanding the uncertainties

Future climate-change impacts and risks are determined by the extent to which the global surface will warm during the 21st century. Projected climatic changes are determined by the amount of greenhouse gases emitted and by how the climate system responds to them (Hausfather and Moore, 2022). However, the anthropogenic signal should be viewed as superimposed on top of natural climate variability, which consists of cycles and fluctuations that occur at all timescales; the natural climate variability occurring from the decadal to the millennial scales is especially important for correctly interpreting the climatic changes observed since 1850 (e.g., Scafetta, 2013, 2021b).

GCM simulations for the 21st century, such as those shown in Fig. 1 (Masson-Delmotte et al., 2021; Pörtner et al., 2022), were used to assess global and regional impacts and risks associated with global warming. Fig. 1 illustrates that the GCM simulations differ significantly both amongst models and because of the chosen SSP scenario adopted for the simulation. The entire ensemble of climate projections estimates that, by 2100, global surface temperatures might rise from 1.3 °C to 8.0 °C, meaning that climate change could have a wide range of effects on civilizations and the environment throughout the 21st century, ranging from beneficial to catastrophic. The main sources of uncertainty are briefly described below.

2.1. The SSP scenarios

The GCM simulations for the 21st century were obtained under different greenhouse gas emission scenarios known as representative concentration pathways (RCPs) and, more recently, five shared socioeconomic pathways (SSPs) describing alternative socioeconomic developments (Riahi et al., 2017). The latter were classified as SSP1 (sustainability), SSP2 (middle of the road), SSP3 (regional rivalry), SSP4 (inequality), and SSP5 (fossil-fueled development). These labels were combined with the expected level of radiative forcing in the year 2100 relative to 1750, which varies from 1.9 W/m^2 to 8.5 W/m^2.

The SSP scenarios explicitly adopted by the IPCC AR6 (Masson-Delmotte et al., 2021) and herein considered are:

- SSP1-2.6 — low GHG emissions and strong adaptation and mitigation (CO_2 emissions are cut to net-zero by 2050–2075); this is a kind of SSP scenarios compatible with the Paris Agreement pledges needed to limit the global surface warming just below the "safe" threshold of 2 °C (Meinshausen et al., 2022) by using the CMIP6 GCMs (Masson-Delmotte et al., 2018; Hausfather et al., 2022; Hausfather and Moore, 2022).
- SSP2-4.5 — intermediate GHG emissions and moderate adaptation and mitigation (CO_2 emission rates remain around current levels until 2050 then they fall but do not reach net-zero by 2100);
- SSP3-7.0 — high GHG emissions and average no policy (CO_2 emissions double by 2100);
- SSP5-8.5 — very high GHG emissions and worst-case no policy (CO_2 emissions triple by 2075).

The likelihood of the aforementioned scenarios were not estimated by the IPCC AR6 (Masson-Delmotte et al., 2021, pp. 54, 231 and 238), despite the fact that having done so would have been essential for properly assessing plausible climate-change impacts and risks. In particular, the SSP5-8.5 scenario produces the most alarming global warming projections ranging from 4 °C to 8 °C by 2100, and it has been the most popular climate scenario used in the scientific literature (Pielke, 2021). For example, the IPCC AR6 (Masson-Delmotte et al., 2021, table 12.12) highlighted the assessments of the emergence of climate impact drivers (CIDs) for the 21st century using the climate simulations derived from the SSP5-8.5 scenario.

However, the choice of highlighting the climate simulations and their risk assessments made with the SSP5-8.5 scenario is questionable because a few authors have investigated the SSP likelihood issue and also the IPCC AR6 briefly acknowledged that "the likelihood of high-emissions scenarios such as RCP8.5 or SSP5-8.5 is considered low in light of recent developments in the energy sector" and that "studies that consider possible future emissions trends in the absence of additional climate policies, such as the recent IEA 2020 World Energy Outlook 'stated policy' scenario (IEA, 2020), project approximately constant fossil fuel and industrial CO_2 emissions out to 2070, approximately in line with the intermediate RCP4.5, RCP6.0 and SSP2-4.5 scenarios" (Masson-Delmotte et al., 2021, pp. 238-239). This is an important statement since the IPCC and many works have considered the SSP5-8.5 extreme scenario to represent the 'business as usual' case (Stocker et al., 2013) despite it was only meant to be a very high-end no-policy scenario (van Vuuren et al., 2011).

In fact, Ritchie and Dowlatabadi (2017) affirmed that the "SSP5-RCP8.5 should not be a priority for future scientific research or a

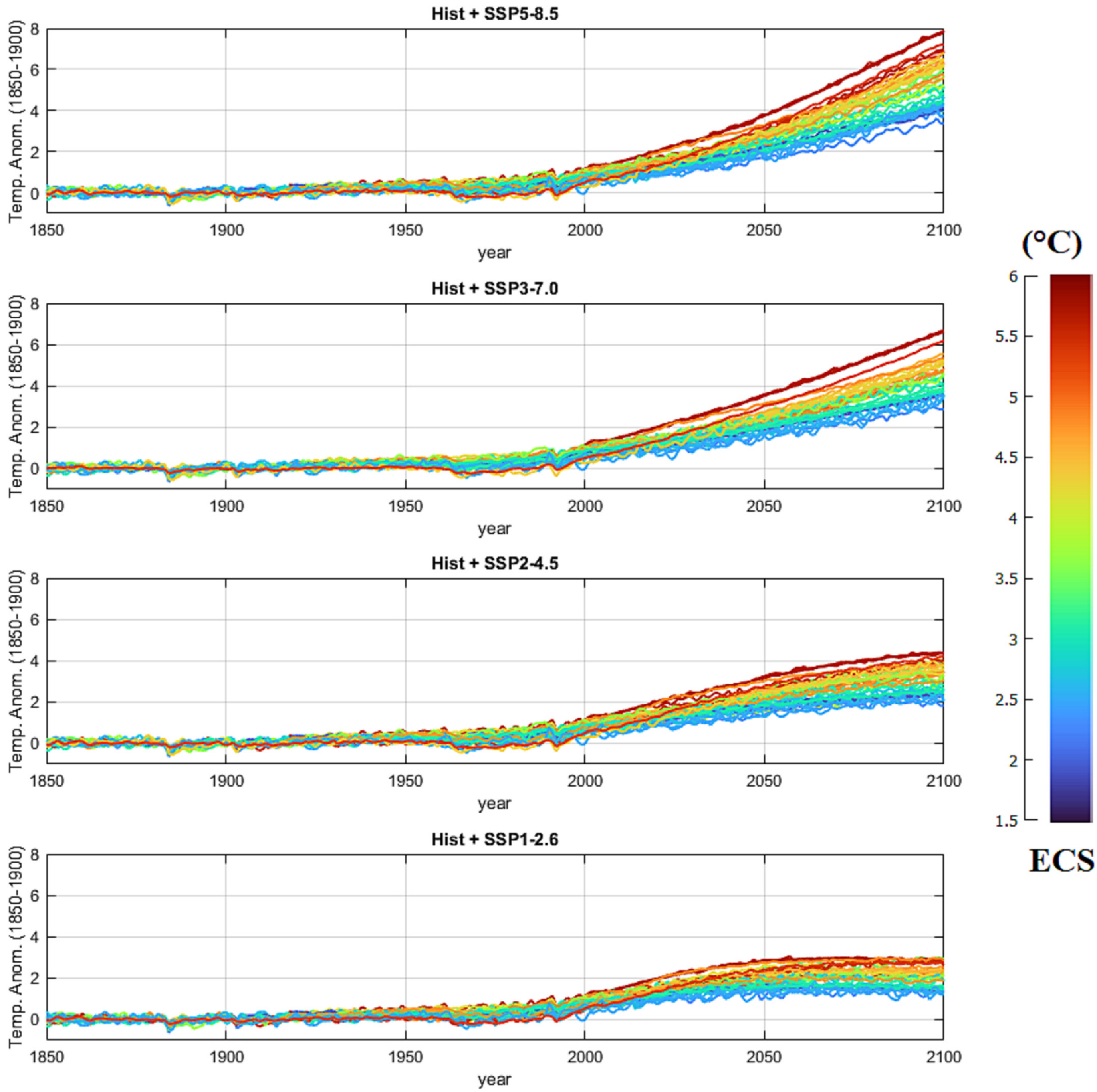

Fig. 1. CMIP6 GCM simulations adopted in the present study (Appendix A). The curve's color scales with the ECS of the models.

benchmark for policy studies"; it is very unlikely because such scenario is based on the implausible assumption of a massive increase of the use of coal that is supposed to substitute all the other forms of energy production. Hausfather and Peters (2020) stated that the "the 'business as usual' story is misleading" and invited researchers "to stop using the worst-case scenario for climate warming as the most likely outcome" because only "more-realistic baselines make for better policy". Hausfather and Peters (2020) described SSP5-8.5 as "highly unlikely", SSP3-7.0 as "unlikely" (as it requires the reversal of some current policies) and SSP2-4.5 as "likely" (because it is the most consistent with current policies).

The SSP5-8.5 and SSP3-7.0 scenarios were also recognized as unrealistic by Burgess et al. (2020) and Pielke and Ritchie (2021a, b), who argued that the IPCC might have misused these scenarios for more than a decade. Pielke et al. (2022) and Burgess et al. (2023) also found that another and even more moderate SSP scenario — the SSP2-3.4, which was ignored by the IPCC AR6 — optimally agrees with the reported emissions from 2005 to 2020 and with the most recent projections of the IEA (2020, 2021) up to 2050. This would imply that the world could be on pace for even more moderate global warming by 2100 than what SSP2-4.5 implies.

For example, SSP3-7.0 and SSP5-8.5 demand that CO_2 atmospheric concentrations climb from around 420 ppm to almost 867 ppm and 1135 ppm, respectively, from 2020 to 2100, which looks to be excessively high; yet, SSP2-4.5 requires a more plausible 602 ppm level by 2100 (Meinshausen et al., 2020). See also

Meinshausen et al. (2023) who reviewed the next generation of Earth system model likely scenarios.

As a result, only the SSP2-4.5 baseline or other even more moderate scenarios (Pielke et al., 2022) could be plausible. Thus, policies aimed to address realistic impacts and risks of climate changes should be based only on such moderate scenarios.

2.2. The GCM climate sensitivity uncertainty

The latest computer climate simulations were generated using the Global Climate Models (GCMs) of the Coupled Model Intercomparison Project phase 6 (CMIP6), which is overseen by the World Climate Research Program (WCRP) of the Working Group on Coupled Modelling (WGCM) (Eyring et al., 2016). More than 50 CMIP6 models exist. These GCMs used historically estimated forcing functions from 1850 to 2014, which were extended from 2015 to 2100 using the estimated forcing functions deduced from the chosen SSP scenarios. The initial conditions and other internal model parameters could be randomly varied within their estimated error ranges to produce ensembles of climate simulations. The impacts and risks of the projected climate changes are typically evaluated for prospective reference periods in the short (2021–2040), mid-term (2041–2060), and long-term (2081–2100). The ensembles of such climate projections were then used for policy planning on adaptation, mitigation, and resilience.

However, as Fig. 1 shows, the CMIP6 GCM simulations produce diverging climate chronologies for the 21st century despite using equivalent forcing functions. This significantly raises the level of uncertainty in calculating the impacts and risks of future climate change; such uncertainty needs to be restricted given the significant societal costs associated with climate policies.

A core issue is that a significant fraction of GCMs appear to be functioning too "hot" (Hausfather et al., 2022), implying that climate change policy should discount climate-change projections from the too-hot models. This problem was also acknowledged in the IPCC AR6 reports where the projections from the evidently too-hot GCMs were not used for impact and risk assessments (Pörtner et al., 2022). In fact, the CMIP6 GCMs suggest that doubling atmospheric CO_2 concentrations from pre-industrial levels (from 280 to 560 ppm) would cause, at equilibrium, a global surface warming ranging from 1.8 °C to 5.7 °C (Masson-Delmotte et al., 2021). ECS values larger than 5 °C, on the other hand, already exceeded those of the previous versions of global climate models (CMIP3 and CMIP5 GCMs) used in the IPCC reports in 2007 and 2013.

Doubling the CO_2 content in the atmosphere results in an increase in radiative forcing of around 3.7 W/m^2, which should cause a global warming of roughly 1 °C according to the Stefan–Boltzmann law (Rahmstorf, 2008). However, the actual warming depends also on the feedback response of the climate system to the applied forcing (Roe, 2009), but the magnitude of such a response is still highly uncertain (Knutti et al., 2017).

There are different definitions of climate sensitivity. The equilibrium climate sensitivity (ECS) is the long-term temperature rise (equilibrium global mean near-surface air temperature) that is expected to result from a doubling of the atmospheric CO_2 concentration (Masson-Delmotte et al., 2021). Once the CO_2 concentration has stopped rising and most of the feedbacks have had time to fully take effect, the model predicts a new global mean near-surface air temperature level. However, after CO_2 has doubled, it can take centuries or even millennia to reach a new equilibrium temperature. Another commonly used definition is the transient climate response (TCR), which is defined as the change in the global mean surface temperature, averaged over a 20-year period, centered at the time of atmospheric CO_2 doubling, in a climate model simulation in which the atmospheric CO_2 concentration increases at 1% per year until it doubles from 280 ppm to 560 ppm (Masson-Delmotte et al., 2021). This means to force the computer climate model with a linearly increasing forcing from 0 to 3.7 W/m^2 for 70 years. As a result, TCR can be assessed using simulations that last a shorter time than those needed to assess ECS. In addition, TCR is smaller than ECS also because slower feedbacks, which might further enhance a temperature increase, require more time to fully respond to an increase in radiative forcing. For instance, after a radiative perturbation, the deep ocean could take several centuries to achieve a new steady state while continuing to cool the top ocean as a heatsink. The CMIP6 GCMs calculate TCR values ranging between 1.2 °C and 2.8 °C. In any case, ECS and TCR values of the CMIP6 GCMs are closely correlated (Scafetta, 2023b).

Estimating the most realistic ECS and TCR ranges, on the other hand, has been a highly controversial topic for more than 140 years because their values strongly dependent on the physical assumptions that one makes, particularly on how the water vapor and cloud feedbacks are treated. For example, Arrenius (1896) estimated that doubling CO_2 could result in a 5–6 °C increase in global surface temperature; however, 10 years later, the same author concluded that his previous estimate was incorrect and proposed lower ECS values ranging from 1.6 °C to 3.9 °C (Arrenius, 1906). Möller (1963) found that the ECS estimate could vary greatly, up to one order of magnitude, according to how water vapor and/or cloudiness responded to the CO_2 perturbation, and concluded that such an uncertainty implied that "the theory that climatic variations are affected by variations in the CO_2 content becomes very questionable". Manabe and Wetherald (1967) developed a one-dimensional climate model and estimated that the ECS could be about 2.0 °C (which was related also to the 2.0 °C target for cost-benefit analyses; Gao et al., 2017). Later, however, with a different model, Manabe and Wetherald (1975) estimated that the likely ECS could be 2.93 °C.

In 1979, the US National Research Council concluded that ECS could likely (or 66%) lie from 1.5 °C and 4.5 °C (Charney et al., 1979). In its two earlier Assessment Reports — FAR (1990) and SAR (1996) — the IPCC concurred and qualitatively estimated that the real ECS value had likely to lie between 1.5 °C and 4.5 °C. In its third Assessment Report, the IPCC changed a little bit the likely range to lie between 1.75 °C and 4.25 °C. In 2007, the IPCC Fourth Assessment Report claimed to have formally quantified the uncertainties and that the likely ECS range was to lie between 2 °C and 4.5 °C. In 2013, however, the IPCC Fifth Assessment Report claimed again that the ECS likely range had to be between 1.5 °C and 4.5 °C. By accepting the analysis by Sherwood et al. (2020) on the assessment of the Earth's climate sensitivity to radiative forcing using multiple lines of evidence, the latest Assessment Report of the IPCC (AR6, Masson-Delmotte et al., 2021) concluded that the likely ECS (66% confidence) should lie between 2.6 °C and 3.9 °C, and very likely (90% confidence) between 2.3 °C and 4.7 °C. The likely TCR could range between 1.4 °C and 2.2 °C. Thus, the IPCC AR6 concluded that the ECS likely range had to lie between 2.5 °C and 4.0 °C, and very-likely between 2.0 °C and 5.0 °C. This suggested that to assess climate-related impacts and risks for the 21st century and, as a result, to develop public policies aimed at addressing and/or mitigating them, the CMIP6 GCMs that predicted ECS or TCR values outside of such ranges do not have to be used. Rugenstein et al. (2023) provided an overview of the "best" ECS estimations proposed since 1979 to the present, all of which offer extremely broad uncertainty ranges.

However, as additional studies were concluded, in time the task of determining the actual ECS has grown more and more compelling. In fact, Knutti et al. (2017) stressed that not only the scientific literature proposes ECS values ranging from 0.5 °C to 6.0 °C or even within a wider range, but that "evidence from climate modelling favours values of ECS in the upper part of the 'likely' range, whereas many recent studies based on instrumentally recorded warming — and some from palaeoclimate — favour values in the lower part of the range". Rugenstein et al. (2023) confirmed the conundrum by stating: "Early in the 2010s, a substantial discrepancy was noted between estimates of climate sensitivity derived from climate models and estimates based on the observed warming record and radiative balance ... Estimates based on observed warming pointed to much lower values than those derived from models". Such conclusions indicate that there is a substantial dichotomy between empirical and GCM studies regarding the actual climate sensitivity to radiative forcing, which is likely owing to the GCMs' inability to adequately hindcast natural climate variability and its geographic patterns. The dilemma is serious since, according to the scientific method, conclusions based on empirical data should be given preference, but the IPCC and climate policies rely on impact and risk assessments derived from questionable GCM projections. For example, Mauritsen et al. (2019) and Mauritsen and Roeckner (2020) demonstrated that by slightly altering the free parameters that regulate the cloud feedback, the model ECS could be reduced from 7 °C to roughly 3 °C, effectively halving the expected global warming by 2100.

Several recent attempts have been made to better constrain the ECS likely range. For example, Nijsse et al. (2020) derived that the likely ECS range should be 1.9–3.4 °C and Lewis (2023) directly challenged the assessments proposed by Sherwood et al. (2020), which were adopted by the IPCC (Masson-Delmotte et al., 2021). Lewis' corrections and revisions of the methodologies used by Sherwood et al. (2020) lead to a likely (17%–83%) ECS range between 1.75 °C and 2.7 °C and a 5%–95% range between 1.55 °C and 3.2 °C. Scafetta (2021c, 2022, 2023a,b) tested how well the CMIP6 GCMs hindcast the global surface warming observed from 1980 to 1990 to 2011–2021 in function of their ECS and TCR values. Such a period was chosen because it is claimed to be characterized by climate records with the smallest uncertainty and, moreover, both surface and satellite records are available for comparison and alternative interpretations. It was discovered that, as climate sensitivity to radiative forcing diminishes, the performance of the CMIP6 GCMs improves. By aggregating the CMIP6 GCMs into three sub-ensembles (herein labeled "macro-GCMs") according to their ECS value — low-ECS (1.5 °C < ECS ≤ 3.0 °C), medium-ECS (3.0 °C < ECS ≤ 4.5 °C), and high-ECS (4.5 °C < ECS ≤ 6.0 °C) — only the low-ECS macro-GCM was found to produce a warming of 0.60 °C ± 0.12 °C, which hindcasts sufficiently well the 0.5–0.6 °C warming observed in various global surface temperature records (Ishihara, 2006; Morice et al., 2012; Lenssen et al., 2019; Hersbach et al., 2020, 2021; Rohde and Hausfather, 2020; Zhang et al., 2019). On the contrary, the medium and high-ECS macro-GCMs produced a warming of 0.79 °C ± 0.10 °C and 0.94 °C ± 0.23 °C, respectively, which consistently showed a warm bias, suggesting that these two macro-GCMs may not be reliable climate predictors for climate-change policies for the 21st century. Also Spencer and Christy (2023) found that the actual value of the ECS should be on the lower end of the range produced by current GCMs and, therefore, confirmed Scafetta (2022). It is worth noting that Schmidt et al. (2023)'s critique of Scafetta (2022) was refuted because it was shown to be based on statistical and physical flaws (Scafetta, 2023d).

Thus, current research suggests that only the low-ECS macro-GCM could be used for assessing the impacts and risks of climate change for the 21st century because the actual ECS should be lower than about 3 °C while the IPCC AR6 assumed an ECS likely range between 2.5 °C and 4.0 °C.

2.3. The surface and satellite 1980–2022 global warming divergence

Scafetta (2023a,b) also argued that even the low-ECS macro-GCM should be considered too hot if the 0.4 °C of warming reported by the UAH-MSU satellite lower troposphere (lt) global temperature record (Spencer et al., 2017) from 1980–1990 to 2011–2021 accurately represents actual surface warming better than what global surface temperature records claim. In fact, McKitrick and Christy (2020) and Mitchell et al. (2020) discovered that all CMIP6 GCMs appear to be affected by a strong warm bias throughout the troposphere, particularly above the tropics, where the models hindcast a hotspot at roughly 10 km height that is not observed in the data. The difference in model and satellite tropospheric warming rates was acknowledged by Santer et al. (2017) and is also reported by the IPCC AR6 (Masson-Delmotte et al., 2021, figure 3.10). The logical conclusion would be that the actual ECS value could be at or below the bottom of the CMIP6 GCM range, that is below about 2 °C, which would imply an even lower projected warming for the 21st century.

In general, according to the atmospheric physics used in the models, the troposphere should warm quicker than the surface since greenhouse gases are expected to warm the troposphere first by activating water vapor and negative lapse rate feedbacks. As a result, the warming of the lower troposphere should be larger, not smaller, than the warming at the surface. Thus, if the surface warming of the Earth were caused by greater greenhouse gas concentrations, as the GCMs suggest, the warming rate in the lower troposphere can be viewed as the upper limit of the possible warming rate at the surface.

The discrepancy between satellite-based and surface-based surface temperature data could be due to non-climatic warm biases generated by contamination from urban heat island (UHI) or other local non-climatic warming sources existing on the surface. In fact, Scafetta and Ouyang (2019) and Scafetta (2021a) demonstrated that non-climatic warming biases could affect extended land regions because, in comparison to GCM simulations, nocturnal minimum temperatures warmed too quickly relative to diurnal maximum temperatures, even in already homogenized temperature records. Furthermore, comparisons of surface temperature records between GCM simulations and lower troposphere UAH-MSU satellite measurements revealed that the land region warmed far more quickly than the ocean region. By contrast, the warming of the ocean area is roughly replicated by the satellite microwave derived temperatures (Scafetta, 2021a, 2023a,b). Scafetta (2021c) also investigated and compared alternative surface temperature data (ERA5-T2m, HadCRUT4, GISTEMP 250 km, NOAA v5) utilizing regional distributions of warming patterns from 1980–1990 to 2011–2021; it was discovered that the land regions were frequently much warmer than what the UAH-MSU v. 6.0 lt and the ERA5 t850 temperature records revealed. There exists also a so-called "divergence problem", in which proxy temperature records based on three-ring width chronologies show much less warming than the temperature data from land stations of similar latitudes since the 1970s (Spencer et al., 2017; Büntgen et al., 2021), which further suggests a non-climatic warm bias affecting global surface temperature records (Spencer et al., 2017; Büntgen et al., 2021). Indeed, Connolly et al. (2021) and Soon et al. (2023) showed that a Northern Hemisphere land surface temperature record derived entirely from confirmed rural-only stations demonstrates up to 40% less warming relative to the preindustrial period (1850–1900) than records derived from both urban and rural stations. Additional studied on a significant UHI influence on the surface temperature records are being conducted (Spencer, 2023).

Scafetta (2023b, figure 5F) also compared three consecutive versions of the HadCRUT global surface temperature records — HadCRUT3 (discontinued after May 2014), HadCRUT4 (discontinued after December 2021), and non-infilled data and infilled HadCRUT5 (the most recent version) — and discovered that the global surface temperature warming trend since 2000 has been progressively increased by consecutive adjustments of the data. The

2000–2014 temperature "pause" or "hiatus", which was clearly visible in HadCRUT3 and acknowledged by the IPCC AR5 (Stocker et al., 2013), has now completely disappeared in the infilled HadCRUT5 record, which adopts model predictions for filling the regional and temporal gaps in the observations. This situation cannot be explained simply as the result of optimized temperature data because the lower troposphere satellite microwave derived temperature records (UAH-MSU v6) still indicate a significant "pause" from 2000 to 2014. The same is true for Connolly et al. (2021) and Soon et al. (2023)'s rural-only derived surface temperature record: see Scafetta (2023b, figure 5B). It is possible that the new adopted homogenization algorithms added some spurious warming to the land records as a result of a mathematical artifact known as "urban blending" (O'Neill et al., 2022; Katata et al., 2023), and/or the models used to fill in the temporal and areal data gaps introduced some spurious warming because of the warming bias that the climate models present.

It should, however, be noticed that the satellite-based UAH-MSU lt temperature record by Spencer et al. (2017) was deemed controversial because, after some data adjustments made in 2014 in the remote sensing system (RSS), the RSS alternative lower troposphere global temperature record by Mears and Wentz (2016) showed a warming trend that appeared more compatible with those presented by the surface-based temperature records; the NOAA-STAR v. 4.0 troposphere temperature dataset presented trends similar to RSS (Santer et al., 2017) and, therefore, yielded a similar conclusion contradicting UAH-MSU. However, Zou et al. (2023) recently revised the NOAA-STAR troposphere temperature records by addressing certain errors in their previous version. The new NOAA-STAR v. 5.0 troposphere records now closely reflect and, therefore, confirms the lower warming trend of the UAH-MSU temperature records. The discovery adds to the growing body of evidence that global surface temperature data are warm-biased, as the CMIP6 GCMs predict that a GHG increase should warm the troposphere faster than the surface.

2.4. Issues related to the natural climate variability not reproduced by the GCMs

Climate records are characterized by large secular and millennial oscillations throughout the Holocene (e.g.: Alley, 2000; Bond et al., 2001; Neff et al., 2001; Kutschera et al., 2017), with the millennial ones responsible for well documented warm periods such as the Roman (approximately 2000 years ago) and Medieval (around 1000 years ago) ones (Ljungqvist, 2010; Christiansen and Ljungqvist, 2012; Luterbacher et al., 2016; Lasher and Axford, 2019; Büntgen et al., 2021). Moreover, spectral examinations of global (land and ocean) surface temperature data show that the climate system is characterized by a significant number of distinct natural oscillations (for example, with periods of roughly 5.2, 5.9, 6.6, 7.4, 9.1, 10.5, 14, 20 and 60 years) (Scafetta, 2010, 2013, 2021b). The quasi 60-year oscillation appears to be rather important and is found in a vast range of climatic datasets such as global sea level, Atlantic Multidecadal Oscillation (AMO), and North Atlantic Oscillation (NAO) records dating back for centuries and millennia (Knudsen et al., 2011; Wyatt and Curry, 2013; Scafetta, 2014a). The Holocene also experienced a Climate Optimum, particularly in the Northern Hemisphere, between roughly 9500 and 5500 years ago, with a thermal maximum around 8000 years ago, which is not reproduced by models, indicating the need to improve our understanding of natural climate forcings and feedbacks, as well as their representation in GCMs (Kaufman and Broadman, 2023).

The quasi millennial and 60-year oscillations appear to have been responsible for at least 50% of the 1900–2000 and 1970–2000 warming, respectively. The latter was also responsible for the substantial warm period that occurred in the 1940s and subsequent cooling observed globally from the 1940s to the 1970s (Scafetta, 2010, 2013). It has been observed that a synchronous quasi-60-year modulation appears in specific solar activity reconstructions over the last 150 years that closely match the quasi-60-year modulation observed in climate data (Connolly et al., 2023; Scafetta, 2023c; Soon et al., 2023). In general, all climatic oscillations from the inter-annual to the multi-millennial timescales appear to be spectrally coherent with solar and/or astronomical oscillations (Eddy, 1976; Kerr, 2001; Neff et al., 2001; Kirkby, 2007; Scafetta, 2010, 2014b, 2020; Steinhilber et al., 2012; Czymzik et al., 2016; Schmutz, 2021; Scafetta and Bianchini, 2023; and many others).

Scafetta (2012a, 2013, 2021b) demonstrated that the GCMs are unable to reproduce these natural oscillations and, as a result, they incorrectly attribute nearly 100% of the global surface warming observed during 1850–1900 to the present and, in particular, that observed from the 1970s to the 2000s, to anthropogenic greenhouse emissions. Indeed, it appears that the millennial natural oscillation has been warming the climate system since 1700, that is since the coldest era of the Little Ice Age, and may have been responsible for a large percentage of the global surface warming of the twentieth century.

For example, figure 3.2 of the IPCC AR6 (Masson-Delmotte et al., 2021, p. 432) highlights the inability of the CMIP6 climate models to hindcast the Medieval Warm Period, which normally lasted from roughly 800 to 1350. Thus, these models are not able to reproduce the millennial oscillation. In fact, the IPCC AR6 (p. 433) explicitly acknowledges that "before the year 1300" there are "larger disagreements between models and temperature reconstructions" even by using the paleoclimate reconstruction proposed by the PAGES2k Consortium (2017), which appears to attenuate the Medieval Warming in comparison to other paleotemperature reconstructions (e.g.: Moberg et al., 2005; Loehle and McCulloch, 2008; Mann et al., 2008; Ljungqvist, 2010; Christiansen and Ljungqvist, 2012; Luterbacher et al., 2016; Ge et al., 2017; Kutschera et al., 2017; Lüning et al., 2019) as those reported by the IPCC AR5 (Stocker et al., 2013, figure 5.7a). The IPCC AR6 is ambiguous on the physical cause of such disagreements by stating (p. 433) that they could just "be expected because forcing and temperature reconstructions are increasingly uncertain further back in time (specific causes have not yet been identified conclusively)". More specifically, AR6 did not acknowledge that several empirical studies have already suggested that the cause could have been a Medieval high solar activity (Eddy, 1976; Bond et al., 2001; Kerr, 2001; Kirkby, 2007; Steinhilber et al., 2012; Scafetta, 2013; Scafetta and Bianchini, 2023), whose real effect on the climate could not be reproduced by the CMIP6 models.

Several authors proposed empirical models for global climate change based on the above results. Here I will review the main model that I proposed because it passed several tests (Scafetta, 2010, 2013, 2021c, 2023c). The empirical modeling of natural climate oscillations not reproduced by the GCMs suggests that the climate system is significantly less sensitive to variations in greenhouse gas concentrations while being significantly oversensitive to variations in solar activity changes. I estimated that the actual ECS could be between 1 °C and 2 °C. Equally low ECS estimates were also found by others (Lindzen and Choi, 2011; Monckton et al., 2015; Bates, 2016; McKitrick and Christy, 2020; Stefani, 2021).

The climate system could appear to be over-sensitivity to solar activity changes because the Sun should impact climate change not only through total solar irradiance (TSI) variations, as the GCMs assume, but also through variations in its ultraviolet light and magnetic field. UV forcing directly modifies stratospheric ozone, whereas solar magnetic activity modifies fluxes of interplanetary charged particles – cosmic rays, solar wind, and interplanetary dust – that could directly influence the electric properties of the atmosphere and its cloud system (Scafetta, 2023c; Scafetta et al., 2016; Shaviv, 2002; Svensmark et al., 2016; Scafetta et al., 2020; Svensmark, 2022). In particular, Scafetta (2023c) showed that direct TSI forcing could even explain only 20% of the total solar effect on climate change. That TSI variations by alone cannot explain how to Sun could modulate the atmosphere of a planet was recently demonstrated by Chavez et al. (2023), who discovered that, despite Neptune being 30 times farther from the Sun than Earth, its cloud activity exhibits a remarkable relationship with the 11-year solar activity cycles; the (still unknown) physical mechanism could not be TSI variations since on Neptune the latter are 900 times smaller than on Earth.

Furthermore, it should be noticed that the CMIP6 GCMs minimize the solar effect on the climate also because they use a solar forcing derived from a specific TSI reconstruction which presents a very little and nearly constant secular variability (Matthes et al., 2017), although the scientific literature also recommends other TSI reconstructions that show a much larger secular variability (e.g., Hoyt and Schatten, 1993; Egorova et al., 2018; Penza et al., 2022) and that also appear to be better correlated with uncontroversial TSI satellite measurements (Scafetta et al., 2019; Connolly et al., 2021; Scafetta, 2023c). Also the CMIP6 models used for the millennial simulation were forced with a very low variability TSI reconstruction such as the PMIP4 SATIRE-M (Wu et al., 2018), which could be erroneous because several other TSI reconstructions exist and show a much larger secular and millennial variability (Scafetta et al., 2019; Connolly et al., 2023; Scafetta, 2023c). In particular, Scafetta (2021b, figure 7) explicitly demonstrated that the GCMs cannot reproduce the Medieval Warm Period (and likely any other warm periods of the Holocene) because they assume only a nearly constant radiative solar forcing and, therefore, there is no net radiative forcing capable of reproducing a significant warming during the Medieval period because volcanic forcing is sporadic and anthropogenic forcing is also absent. This (apparently arbitrary) choice taken by the CMIP6 GCM modelers regarding solar forcing also contributes to both the GCMs' high ECS values (which are required to reconstruct the 20th-century warming using anthropogenic forcing alone) and to their failure in reconstructing the other warm periods of the Holocene.

See Connolly et al. (2021), Scafetta (2023c) and Soon et al. (2023) for additional commentary, modeling and supporting bibliography regarding how to empirically assess the role of the Sun in climate change using various multi-proxy solar records.

3. Addressing the "too hot" model problem

As discussed in Section 2, a number of evidence point to the conclusion that at least the majority of CMIP6 GCMs are running too hot, even more than what the IPCC (Masson-Delmotte et al., 2021) and Hausfather et al. (2022) have already admitted. These findings suggest that the CMIP6 GCM climate sensitivity to radiative forcings is significantly overestimated. The CMIP3 and CMIP5 GCMs were already running too hot (Scafetta, 2012a, 2013), but the situation has gotten so critical with the CMIP6 GCMs that also the UN climate panel has raised concerns (Voosen, 2019, 2021).

The most recent research on direct comparison of the CMIP6 GCM hindcasts with global surface temperature records since 1980 indicates that, at most, only the CMIP6 GCMs with low climate sensitivity (e.g. for ECS ≤ 3 °C) could adequately hindcast the observed warming since 1980 and could be used to evaluate the risk associated with projected climate changes for the 21st century (Scafetta, 2022, 2023a,d). Other authors have reached the same result (Lewis, 2023; Spencer and Christy, 2023). Furthermore, various evidences suggest that actual global warming since 1980 may have been less than what is generally reported by the global surface temperature records (Scafetta, 2023b). If this is the case, even the low-ECS CMIP6 macro-GCM would be functioning too hot, rendering all CMIP6 GCMs untrustworthy for guiding public policy targeted at addressing the impacts and risks of projected climate changes for the 21st-century. Finally, alternative climate modeling based on actual evidence of underestimated natural cycles and solar influences also suggests low ECS values to radiative forcing. In fact, according to these evidences, the true ECS may likely be in the range of 1–2 °C (e.g.: Scafetta, 2013, 2021b, 2023c; Scafetta and Bianchini, 2023).

In the following, this paper assesses the impacts and risks of climate change suggested by the IPCC (Pörtner et al., 2022) using the SSP2.4.5 scenario and the 21st century warming projected by the low-ECS CMIP6 macro-GCM. Alternative calculations account for the possibility that even the low sensitivity models are running too hot because, based on satellite low troposphere temperature records, the actual 1980–2022 warming may be less than what claimed in Masson-Delmotte et al. (2021). Finally, alternative risk assessments are provided by employing the empirical global surface temperature models for the 21st century proposed by Scafetta (2013, 2021b).

4. Re-assessment: selection of reliable GCMs

Climate simulations from 42 CMIP6 GCMs are analyzed here. The computer simulations were created using historical forcings (1850–2014) further extended up to 2100 with hypothetical forcing functions deduced from four different SSP scenarios: SSP1-2.6 (low GHG emissions), SSP2-4.5 (intermediate GHG emissions), SSP3-7.0 (high GHG emissions) and SSP5-8.5 (very high greenhouse gas emissions). These four scenarios are nearly indistinguishable until 2022. Thus, from 1850 to 2022, the four simulation ensembles can be considered independent assessments of the same models under nearly identical forcing conditions. This variability also helps to assess in first approximation the spreading related with the chaotic internal variability of the models: see also Scafetta (2023a) where the GCM internal variability issue is extensively discussed.

A total of 156 simulations were analyzed. 142 simulations were "average" records provided by the Koninklijk Nederlands Meteorologisch Instituut (KNMI) Climate Explorer (van Oldenborgh, 2020). Other 14 simulations were missing in Climate Explorer and were taken from the supplementary of Hausfather et al. (2022). The latter include those produced by four GCMs: CMCC-ESM2, GFDL-CM4, IITM-ESM and TaiESM1. The ECS and TCR values of the GCMs were taken from table 7.SM.5 of the IPCC AR6 (Masson-Delmotte et al., 2021). Some missing values were taken from the supplementary of Hausfather et al. (2022). The ECS of FIO-ESM-2-0 was hypothesized to be 4.27 °C because its TCR falls between those of CNRM-CM6-1 and EC-Earth3.

Table 1 lists the adopted GCMs with their estimated ECS and TCR values, which are approximately correlated to each other (Scafetta, 2023b). The GCMs are also grouped in three macro-GCMs according to their ECS value: low-ECS (1.5 °C < ECS ≤ 3.0 °C); medium-ECS (3.0 °C < ECS ≤ 4.5 °C), and high-ECS (4.5 °C < ECS ≤ 6.0 °C), as already proposed by Scafetta (2023b,a, 2022).

Fig. 1 shows the adopted 156 CMIP6 GCM simulations which are baselined in 1850–1900. The curve's color scales with the ECS value of the models from blue (low sensitivity) to red (high sensitivity). The figure shows that, as the ECS increases, the warming projected by the models during the 21st century tends to increase as well. Similar results can be obtained by coloring the curves in function of the TCR value of their GCM.

Table 1
CMIP6 GCMs analyzed in the present study. They are ranked according to their ECS (left) and TCR (right) values. (The ECS of FIO-ESM-2–0 is hypothesized).

Macro-GCM	Model Name	ECS (°C)	Macro-GCM	Model Name	TCR (°C)
High-ECS	CIESM	5.63	High-TCR	UKESM1-0-LL f2	2.79
	CanESM5 p1	5.62		CanESM5 p1	2.74
	CanESM5 p2	5.62		CanESM5 p2	2.74
	CanESM5-CanOE p2	5.62		CanESM5-CanOE p2	2.74
	HadGEM3-GC31-LL f3	5.55		NESM3	2.72
	HadGEM3-GC31-MM f3	5.42		EC-Earth3-Veg	2.62
	UKESM1-0-LL-f2	5.34		HadGEM3-GC31-MM-f3	2.58
	CESM2	5.16		HadGEM3-GC31-LL-f3	2.55
	CNRM-CM6-1-f2	4.83		CNRM-CM6-1-HR-f2	2.48
	CNRM-ESM2-1-f2	4.76		CIESM	2.39
	CESM2-WACCM	4.75		TaiESM1	2.34
	KACE-1–0-G	4.75		IPSL-CM6A-LR	2.32
	ACCESS-CM2	4.72	Medium-TCR	EC-Earth3	2.30
	NESM3	4.72		FIO-ESM-2–0	2.22
	IPSL-CM6A-LR	4.56		CNRM-CM6-1 f2	2.14
Medium-ECS	EC-Earth3-Veg	4.31		ACCESS-CM2	2.10
	TaiESM1	4.31		CMCC-CM2-SR5	2.09
	CNRM-CM6-1-HR f2	4.28		AWI-CM-1–1-MR	2.06
	FIO-ESM-2–0	4.27		CESM2	2.06
	EC-Earth3	4.26		KACE-1–0-G	2.04
	GFDL-CM4	3.89		GFDL-CM4	2.00
	ACCESS-ESM1-5	3.87		CESM2-WACCM	1.98
	MCM-UA-1–0	3.65		ACCESS-ESM1-5	1.95
	CMCC-ESM2	3.58		FGOALS-f3-L	1.94
	CMCC-CM2-SR5	3.52		MCM-UA-1–0	1.94
	AWI-CM-1–1-MR	3.16		CMCC-ESM2	1.92
	MRI-ESM2-0	3.15		CNRM-ESM2-1 f2	1.86
	BCC-CSM2-MR	3.04		MPI-ESM1-2-LR	1.84
Low-ECS	FGOALS-f3-L	3.00	Low-TCR	GISS-E2-1-G p3	1.80
	MPI-ESM1-2-LR	3.00		CAMS-CSM1-0	1.73
	MPI-ESM1-2-HR	2.98		BCC-CSM2-MR	1.72
	FGOALS-g3	2.88		IITM-ESM	1.71
	GISS-E2-1-G p3	2.72		MPI-ESM1-2-HR	1.66
	MIROC-ES2L f2	2.68		MRI-ESM2-0	1.64
	GFDL-ESM4	2.65		GFDL-ESM4	1.63
	MIROC6	2.61		MIROC-ES2L f2	1.55
	NorESM2-LM	2.54		MIROC6	1.55
	NorESM2-MM	2.50		FGOALS-g3	1.54
	IITM-ESM	2.37		NorESM2-LM	1.48
	CAMS-CSM1-0	2.29		INM-CM5-0	1.41
	INM-CM5-0	1.92		INM-CM4-8	1.33
	INM-CM4-8	1.83		NorESM2-MM	1.33

Fig. 2 shows the adopted 156 CMIP6 GCM simulations, which are now baselined in 1980–1990 to better assess their performance since 1980, when satellite temperature records are also available. The data from the three macro-GCMs are displayed on the three panels. The synthetic records are contrasted to the HadCRUT v. 5.0 global surface temperature (infilled data, which present the most warming of any other HadCRUT records) and the satellite-based UAH-MSU lt v. 6.0 (Spencer et al., 2017), which grows warmer significantly less.

The warming from 1980–1990 to 2011–2022 shown by the (infilled) HadCRUT5 record is nearly identical to that from other global surface temperature records: ERA5-T2m (Hersbach et al., 2020), GISTEMP (Lenssen et al., 2019), and Berkeley Earth Land/Ocean temperature (Rohde and Hausfather, 2020). Instead, the warming presented by the UAH-MSU lower troposphere temperature record is nearly identical to that shown by the recent NOAA-STAR v. 5.0 one (data from Zou et al., 2023).

Fig. 2 reveals that, since 1980, simulations from the medium and high-ECS macro-GCMs appear to be too hot. However, also the low-ECS macro-GCM appears to produce too hot simulations in comparison with the satellite UAH-MSU lt record. These results are confirmed also by considering the 688 GCM individual ensemble simulations available on Climate Explorer (see Scafetta, 2023a, figures 1 and 2).

Fig. 3 confirms the above expectations by using the same approach proposed by Scafetta (2022, 2023a,b). It shows the temperature changes from 1980–1990 to 2012–2022 produced by the adopted 42 GCMs against the correspondent warming shown by HadCRUT v. 5.0 (0.605 °C ± 0.02 °C, 95% confidence) and UAH-MSU lt v. 6.0 (0.432 °C ± 0.03 °C, conjectured 95% confidence). The top panel shows the results against the ECS ranking; the bottom panel shows the same against the TCR ranking. The figure demonstrates that, as ECS or TCR increase, the warming hindcasted by the GCMs increases as well. The GCM results are listed in Table 2, which also reports the [2.5%, 17%, 50%, 83%, 97.5%] percentiles for each macro-GCM.

Only the low-ECS macro-GCM (1.5 °C < ECS $\leq$ 3.0 °C and 1.3 °C < TCR $\leq$ 1.8 °C) appears to generate a distribution of hindcasts that best incorporates the observed warming. These ECS and TCR ranges significantly restrict those of the CMIP6 GCMs (1.5–6.0 °C and 1.3–2.8 °C, respectively) and are compatible with those estimated by Lewis (2023). However, if the actual global warming from 1980 to 2022 is compatible with that shown by the lower troposphere estimates of UAH-MSU v. 6.0, Fig. 3 indicates that even the low-ECS macro-GCM would be running too hot (cf. McKitrick and Christy, 2020). Each model is represented by four separate simulations (where available), which provide a first order estimate of the dispersion due to the models' internal variability.

Fig. 3 also shows that a few GCMs with medium to high ECS and TCR values may be approaching the observed warming. However, because climate projections are created by multi-model ensembles rather than individual models or simulations, a very tiny number

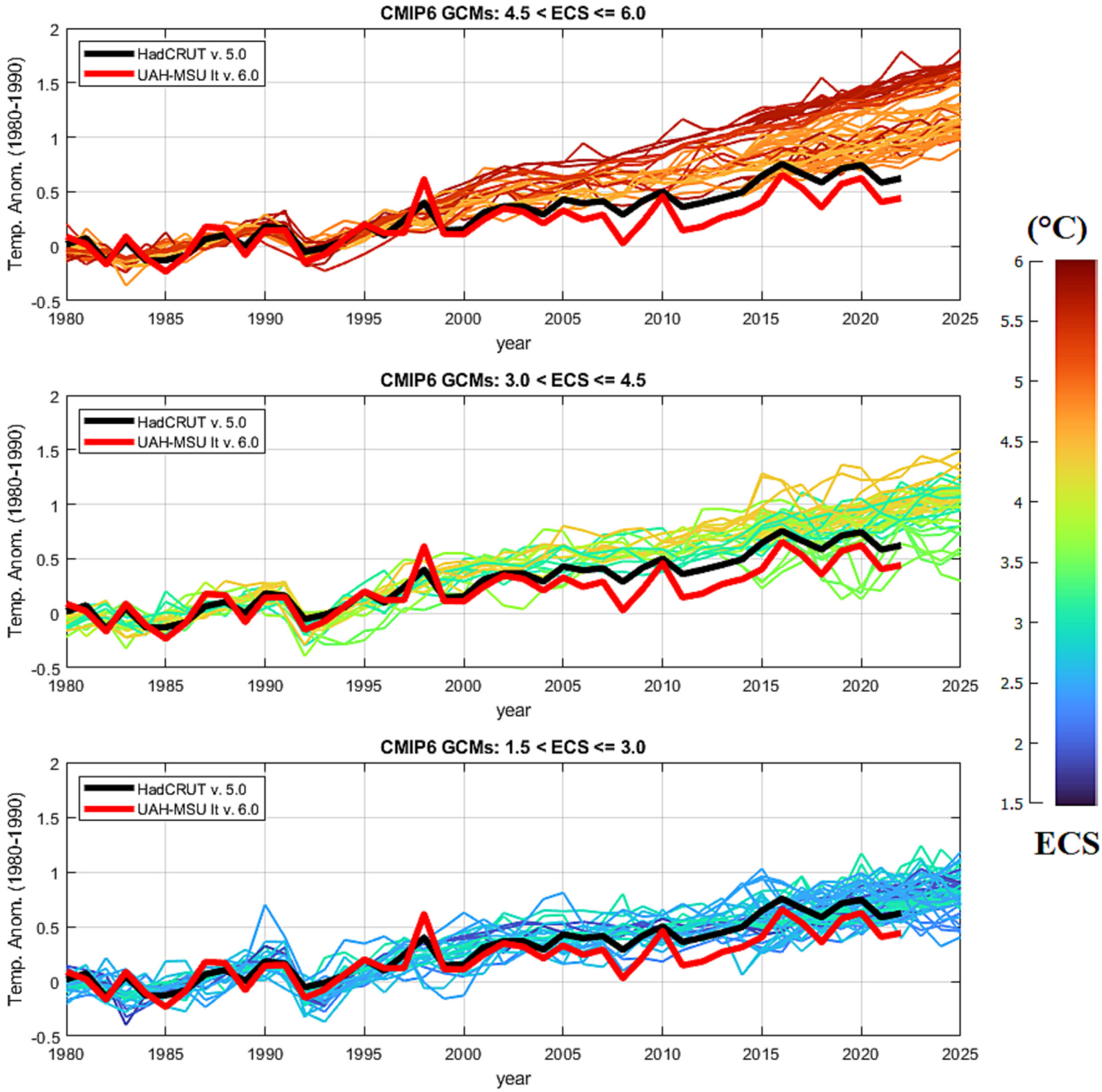

Fig. 2. CMIP6 GCM simulations adopted in the present study divided into three macro-GCMs according to their ECS value. The curve's color scales with the ECS of the models. The synthetic records are compared against the HadCRUT v. 5.0 (infilled data) global surface temperature and the satellite-based UAH-MSU lt v. 6.0 (Spencer et al., 2017).

of favorable instances appearing in the distribution's tails should be statistically classed as outliers. For example, CNRM-ESM2-1 appears to approach the HadCRUT5 warming within the allowed range of ± 0.1 °C (cf. Scafetta, 2023a) only because the model's extraordinarily high ECS (4.76 °C) is compensated by its comparatively low TCR (1.86 °C), which slows down the global surface temperature rise. However, relying on just one GCM to judge whether such a scenario is conceivable would be insufficient; additional GCMs must be created and statistically proven to be consistent with both extremely high ECS values and relatively low TCR values.

Fig. 4 shows boxplots indicating the temperature changes from 1850–1900 to 2040–2060 (left) and 2080–2100 (right) produced the adopted 42 GCMs for the Hist + SSP1-2.6, SSP2-4.5, SSP3-7.0 and SSP5-8.5 emission scenarios. The boxplots indicate the distribution of the GCM forecasts based on a five-number summary ("minimum", first quartile [Q1 = 25%], median [Q2 = 50%], third quartile [Q3 = 75%], "maximum") plus outliers, which are displayed as red crosses. Each line of the figure represents a different selection of GCMs: (i) is based on all CMIP6 GCMs; (ii) uses only the GCMs with ECS ranging between 2.5 °C and 4.0 °C, which corresponds to the IPCC AR6 likely range; (iii) uses only the high-ECS GCMs (4.5 °C < ECS ≤ 6.0 °C); (iv) uses only the medium-ECS CMIP6 GCMs (3.0 °C < ECS ≤ 4.5 °C); (v) uses only the low-ECS CMIP6 GCMs (1.5 °C < ECS ≤ 3.0 °C). Table 3 summaries the quartile statistics of the temperature changes from 1850 to 1900 to 2040–2060 and 2080–2100 produced by the adopted 42 GCMs, similar to that

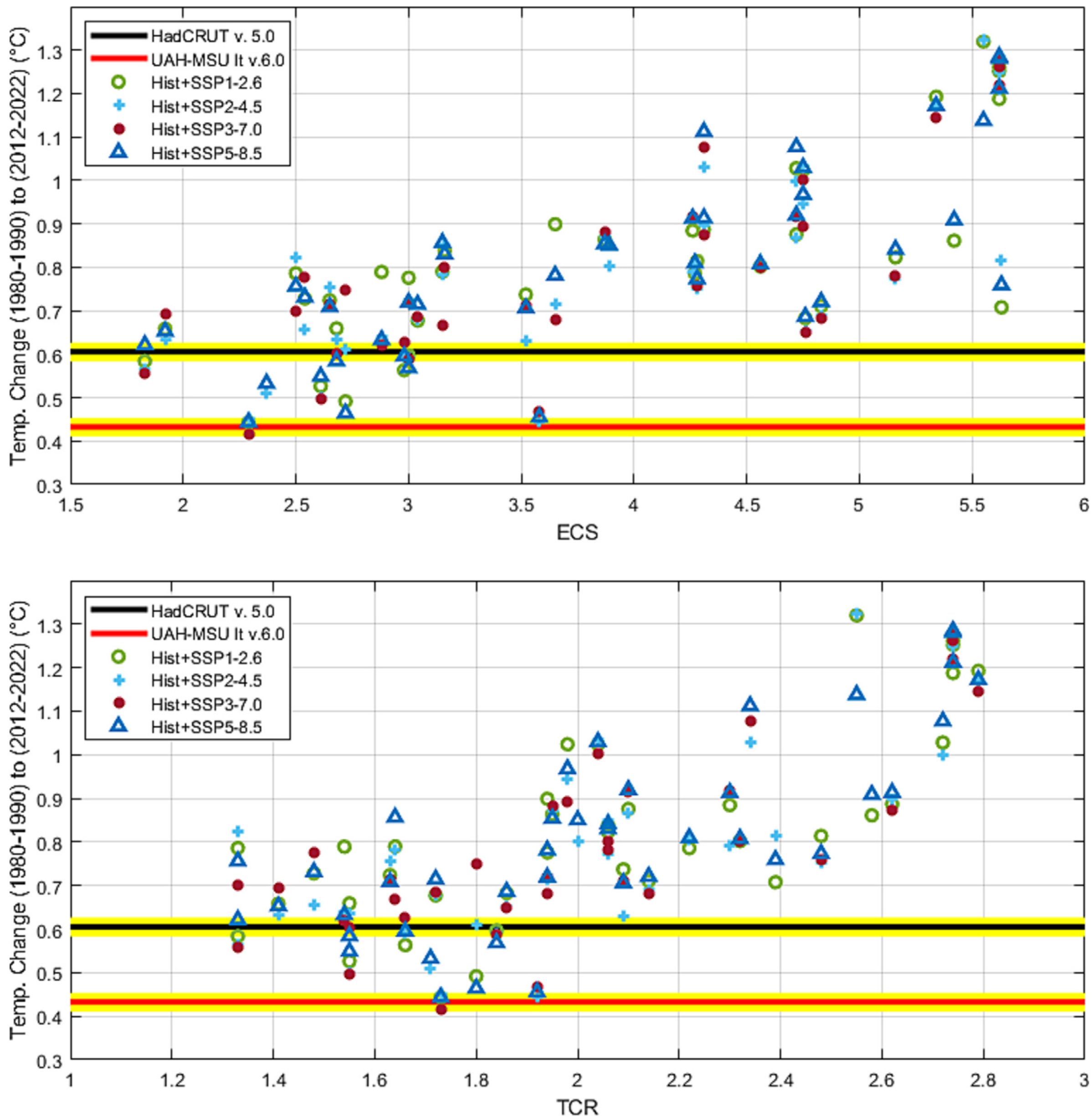

Fig. 3. Temperature changes from 1980–1990 to 2012–2022 produced the adopted 42 GCMs against the warming of HadCRUT v. 5.0 (0.605 °C ± 0.02 °C) and UAH-MSU lt v. 6.0 (0.432 °C ± 0.03 °C): see Table 2. Top: ECS ranking; Bottom: TCR ranking.

produced by the boxplots depicted in Fig. 4 but with a different percentage descriptions [2.5%, 17%, 50%, 83%, 97.5%], which highlights the median, the (likely) 66% and the (very likely) 95% confidence ranges.

For the SSP2-4.5 case, the 2.5–4.0 ECS GCMs project a likely (or 66%) 2080–2100 warming ranging between 2.24 °C and 3.53 °C with median 2.69 °C, which well corresponds to the 2.2–3.4 °C (with median 2.7 °C) range reported by the Climate Action Tracker (2022) as the likely warming that will occur by the end of the 21st century on the basis of real-world current policies.

Fig. 4 shows that the calculated ranges vary greatly according to the adopted SSP scenario and the selection of models used for the simulations. In general, the ensemble of all simulations (apart from those referring to the SSP1-2.6 scenario) appears to easily exceed the 2.0 °C (safe) threshold discussed in Tol (2015) and Gao et al. (2017) by as early as 2050. This would be true whether one chooses to use all CMIP6 GCM simulations or the selection of them that corresponds to the IPCC likely ECS range (between 2.5 °C and 4.0 °C). Only the SSP1-2.6 scenario would ensure an average warming of roughly 1.8 °C [1.26–2.82 °C] by 2080–2100 still using the GCMs corresponding to the IPCC likely ECS-range and could satisfy the Paris Agreement warming target. The SSP1-2.6 scenario is rather aggressive since it requires us to take the "green road" of achieving a net-zero global CO_2 emission condition as soon as 2050, which makes such policy extremely expensive and potentially harmful for society.

However, Fig. 4 and Table 3 suggest that in the eventuality that only the simulations from the low-ECS macro-CGM are considered, also the moderate SSP2-4.5 scenario could be rather feasible for preventing a climatic crisis because by 2050 the average warming will still be < 2.0 °C (roughly 1.77 °C [1.36–2.25 °C]) and by 2080–2100 it will rise to just 2.28 °C [1.96–2.83 °C], instead of 2.69 °C [1.98–3.82 °C] under the IPCC's assumptions. SSP2-4.5 is a "middle of the road" scenario where CO_2 emissions stay about the same as

Table 2
Temperature changes from 1980–1990 to 2012–2022 produced the adopted 42 GCMs, with percentiles for each macro-GCM. NaN indicates missing simulations. (The ECS of FIO-ESM-2-0 is hypothesized).

Model	ECS (°C)	Hist + SSP1-2.6	SSP2-4.5	SSP3-7.0	SSP5-8.5	percentile	°C
High-ECS							
CIESM	5.63	0.71	0.81	NaN	0.76	97.50%	1.31
CanESM5-p1	5.62	1.25	1.25	1.26	1.28	83.00%	1.24
CanESM5-p2	5.62	1.26	1.28	1.28	1.29	50.00%	0.97
CanESM5-CanOE p2	5.62	1.19	1.21	1.22	1.21	17.00%	0.76
HadGEM3-GC31-LL f3	5.55	1.32	1.32	NaN	1.14	2.50%	0.66
HadGEM3-GC31-MM f3	5.42	0.86	NaN	NaN	0.91		
UKESM1-0-LL-f2	5.34	1.19	1.17	1.14	1.17		
CESM2	5.16	0.82	0.77	0.78	0.84		
CNRM-CM6-1 f2	4.83	0.71	0.69	0.68	0.72		
CNRM-ESM2-1 f2	4.76	0.68	0.65	0.65	0.69		
CESM2-WACCM	4.75	1.02	0.95	0.89	0.97		
KACE-1-0-G	4.75	1.02	1.03	1.00	1.03		
ACCESS-CM2	4.72	0.88	0.87	0.92	0.92		
NESM3	4.72	1.03	1.00	NaN	1.08		
IPSL-CM6A-LR	4.56	0.80	0.80	0.80	0.81		
Medium-ECS							
EC-Earth3-Veg	4.31	0.89	0.90	0.87	0.91	97.50%	1.07
TaiESM1	4.31	NaN	1.03	1.08	1.11	83.00%	0.89
CNRM-CM6-1-HR f2	4.28	0.81	0.75	0.76	0.77	50.00%	0.8
FIO-ESM-2-0	4.27	0.79	0.80	NaN	0.81	17.00%	0.68
EC-Earth3	4.26	0.88	0.79	0.92	0.91	2.50%	0.46
GFDL-CM4	3.89	NaN	0.80	NaN	0.85		
ACCESS-ESM1-5	3.87	0.86	0.87	0.88	0.85		
MCM-UA-1-0	3.65	0.90	0.71	0.68	0.78		
CMCC-ESM2	3.58	NaN	0.44	0.47	0.46		
CMCC-CM2-SR5	3.52	0.74	0.63	0.71	0.71		
AWI-CM-1-1-MR	3.16	0.84	0.85	0.80	0.83		
MRI-ESM2-0	3.15	0.79	0.78	0.67	0.86		
BCC-CSM2-MR	3.04	0.68	0.68	0.68	0.71		
Low-ECS							
FGOALS-f3-L	3.00	0.78	0.72	0.72	0.72	97.50%	0.79
MPI-ESM1-2-LR	3.00	0.60	0.59	0.59	0.57	83.00%	0.73
MPI-ESM1-2-HR	2.98	0.56	0.59	0.63	0.60	50.00%	0.62
FGOALS-g3	2.88	0.79	0.64	0.62	0.63	17.00%	0.53
GISS-E2-1-G p3	2.72	0.49	0.61	0.75	0.46	2.50%	0.44
MIROC-ES2L f2	2.68	0.66	0.63	0.60	0.58		
GFDL-ESM4	2.65	0.72	0.76	0.72	0.71		
MIROC6	2.61	0.53	0.50	0.50	0.55		
NorESM2-LM	2.54	0.73	0.66	0.78	0.73		
NorESM2-MM	2.50	0.79	0.82	0.70	0.76		
IITM-ESM	2.37	NaN	0.51	NaN	0.53		
CAMS-CSM1-0	2.29	0.44	0.45	0.41	0.44		
INM-CM5-0	1.92	0.66	0.63	0.69	0.65		
INM-CM4-8	1.83	0.58	0.56	0.56	0.62		

today until the middle of the 21st century, when they begin to progressively fall but, even by 2100, they do not reach net-zero. Thus, this SSP scenario requires no discernible changes in the historical trends of socioeconomic elements for the next 2–3 decades. Development and income growth are uneven, and sustainability progress is gradual. Adaptation policies are assumed to be adequate to mitigate major climate-related hazards.

The climate change projection ensembles used here primarily come from KNMI Climate Explorer's GCM average simulations for each SSP. A critique could be formulated that the entire ensemble of individual simulations, rather than just the ensemble average simulation or a single member simulation for each model and SSP, should be employed, resulting in larger projection ensembles. The topic is controversial and, in any case, impossible to assess because the number of individual runs for each model varies significantly among models. Scafetta (2023a) for example, emphasized that, because physical models must be both accurate and precise, the main prediction of the models is their average simulation, whereas the error-range from such average should be considered a user requirement rather than a GCM property due to its actual internal variability. The user's acceptable error-range for each model can be bounded to the temperature variability within the decadal-bidecadal scales because the models are supposed to reproduce the longer scales, and this variability was estimated to be of the order of about ± 0.1 °C (Scafetta, 2023a, Appendix). Such error can be statistically ignored because it is significantly smaller than the difference observed among the various GCM average simulations. In fact, also Hausfather et al. (2022) evaluated the projection ensembles using one simulation for each model and SSP, which is what I did here.

5. Re-assessment: adoption of optimized empirical climate models

If the actual global warming from 1980 to 2022 is compatible with that provided by UAH-MSU (or NOAA-STAR v. 5.0) lower troposphere temperature data (Spencer et al., 2017; Zou et al., 2023), the actual impacts and risks connected with predicted twenty-first-century climate changes are much smaller, and the CMIP6 GCM simulations should not be used to make policy. In such instance, all CMIP6 GCMs would be inadequate for accurately esti-

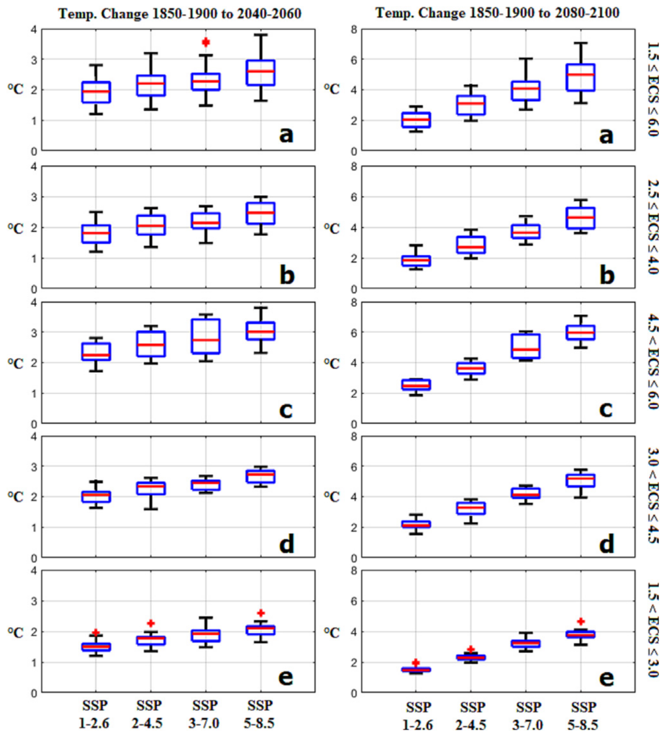

Fig. 4. Boxplots indicating the temperature changes from 1850 to 1900 to 2040–2060 (left) and 2080–2100 (right) produced the adopted 42 GCMs divided for the Hist + SSP1-2.6, SSP2-4.5, SSP3-7.0 and SSP5-8.5 emission scenarios. (a) All CMIP6 GCMs; (b) CMIP6 GCMs with ECS ranging between 2.5 °C and 4.0 °C (the likely IPCC AR6 range); (c) High-ECS CMIP6 GCMs (4.5 °C < ECS ≤ 6.0 °C); (d) Medium-ECS CMIP6 GCMs (3.0 °C < ECS ≤ 4.5 °C); (e) Low-ECS CMIP6 GCMs (1.5 °C < ECS ≤ 3.0 °C).

mating climate changes in the 21st century because the actual ECS would be roughly one-third lower than even the low-ECS macro-GCM, that is between 1 °C and 2 °C (cf. Scafetta, 2013, 2023c; McKitrick and Christy, 2020; Stefani, 2021), which would rule out nearly all CMIP6 GCMs.

There are not enough models that span the ECS range from 1 °C to 2 °C. However, the case could be approximated by empirically scaling the CMIP6 macro-GCM simulations to best reflect the warming documented by satellite data from 1980 to 2022. The purpose is to produce hypothetical GCM simulations that best hindcast the available data, so that their twenty-first-century projections could be trusted for policy.

The proposed scaling algorithm works in first approximation because on a global scale the performance of a GCM is mainly determined by its ECS and TCR values. Moreover, it is easy to calculate that scaling down the medium and high-ECS macro-GCMs to mimic the warming of the low-ECS macro-GCM from 1980–1990 to 2011–2022, the three macro-GCM ensembles would roughly overlap throughout the 21st century. In fact, by using the data from Table 2, the ratio between the 2011–2022 medians of the medium- and high-ECS ensembles and the low-ECS ensemble are 0.80/0.62 ≈ 1.3 and 0.97/0.62 ≈ 1.6, respectively; similar ratios are found using the data from Table 3. By using the 2080–2100 medians: for SSP1-2.6 the ratios are 2.1/1.5 ≈ 1.4 and 2.5/1.5 ≈ 1.7; for SSP2-4.5 the ratios are 3.3/2.3 ≈ 1.4 and 3.6/2.3 ≈ 1.6; for SSP3-7.0 the ratios are 4.1/3.2 ≈ 1.3 and 4.8/3.2 ≈ 1.5; and for SSP5-8.5 the ratios are 5.2/3.7 ≈ 1.4 and 6.0/3.7 ≈ 1.6, respectively. These ratios remain approximately the same for all other percentile levels.

As a result, because the performance of one macro-GCM can be approximated by an appropriate linear scaling of another one, it is legitimate to modify the climate projection ensembles of the available macro-GCMs to generate plausible climate projection ensembles from hypothetical macro-GCMs by scaling them to best reproduce the available data. Another advantage of the proposed methodology is that it can be applied to a wide range of circumstances where the existing GCMs are unsatisfactory. For example, the three proposed macro-GCMs can be scaled to recreate both global surface and lower troposphere temperatures, or they can be scaled and integrated with climate models that empirically recon-

Table 3
Percentile statistics similar to the boxplot statistics depicted in Fig. 4.

		Hist + SSP1-2.6 (°C)		Hist + SSP2-4.5 (°C)		Hist + SSP3-7.0 (°C)		Hist + SSP5-8.5 (°C)	
	percentile	2040–2060	2080–2100	2040–2060	2080–2100	2040–2060	2080–2100	2040–2060	2080–2100
Fig. 4A	97.5%	2.81	2.90	3.19	4.25	3.57	6.03	3.79	7.06
	83.0%	2.40	2.76	2.62	3.72	2.71	4.79	3.03	5.98
	50.0%	1.95	2.04	2.20	3.11	2.28	4.09	2.61	4.99
	17.0%	1.50	1.46	1.70	2.26	1.89	3.22	2.10	3.75
	2.5%	1.22	1.29	1.39	1.97	1.52	2.76	1.71	3.37
Fig. 4B	97.5%	2.49	2.82	2.61	3.82	2.68	4.71	2.98	5.76
	83.0%	2.13	2.32	2.45	3.53	2.52	4.48	2.83	5.43
	50.0%	1.81	1.84	2.04	2.69	2.14	3.64	2.47	4.63
	17.0%	1.43	1.43	1.62	2.24	1.77	3.20	1.98	3.76
	2.5%	1.20	1.26	1.37	1.98	1.49	2.87	1.77	3.63
Fig. 4C	97.5%	2.81	2.91	3.20	4.27	3.58	6.04	3.79	7.07
	83.0%	2.76	2.89	3.16	4.22	3.54	6.00	3.72	6.99
	50.0%	2.25	2.47	2.58	3.62	2.74	4.85	3.01	5.97
	17.0%	1.95	2.20	2.13	3.21	2.25	4.20	2.64	5.45
	2.5%	1.72	1.87	1.98	2.88	2.05	4.14	2.32	4.98
Fig. 4D	97.5%	2.49	2.82	2.62	3.83	2.68	4.72	2.99	5.77
	83.0%	2.36	2.68	2.47	3.64	2.53	4.56	2.91	5.51
	50.0%	2.06	2.11	2.34	3.29	2.45	4.11	2.73	5.19
	17.0%	1.80	1.80	1.99	2.62	2.15	3.74	2.45	4.54
	2.5%	1.64	1.56	1.59	2.25	2.13	3.53	2.33	3.95
Fig. 4E	97.5%	1.95	1.98	2.25	2.83	2.44	3.89	2.58	4.63
	83.0%	1.68	1.69	1.84	2.46	2.11	3.38	2.19	4.00
	50.0%	1.50	1.46	1.77	2.28	1.92	3.23	2.10	3.74
	17.0%	1.28	1.33	1.55	2.11	1.61	2.94	1.85	3.59
	2.5%	1.20	1.26	1.36	1.96	1.48	2.70	1.64	3.12

struct natural cycles and extra solar components that the CMIP GCMs do not reproduce, as Scafetta (2013, 2021b) already proposed.

Let us now address these two situations in detail.

5.1. GCM scaling on the surface and lower troposphere temperature records

As explained in Section 2, climate-change impacts and risks for the 21st century are assessed by the IPCC (Pörtner et al., 2022) using the CMIP6 GCMs simulations under different SSP scenarios. However, Hausfather and Peters (2020) suggested that the SSP2-4.5 scenario is the most plausible. According to Pielke et al. (2022), only the SSP2-3.4 and SSP2-4.5 scenarios should be deemed realistic since their emission trajectories are the most compatible with recent history and present reference estimates of the expected evolution of the global energy system over the next three decades, but here only the SSP2-4.5 GCM simulations are available. Thus, it is here suggested that the Hist + SSP2-4.5 scenario simulations from the CMIP6 GCMs could serve as a basis for realistic climate change projections for the 21st century.

Moreover, according to the analysis presented in Sections 2 and 4, the best-performing subset of CMIP6 GCMs appears to be the one with ECS values between 1.5 °C and 3.0 °C (Lewis, 2023; Scafetta, 2023a). The low-ECS macro GCM is composed of 15 GCMs. From this list it might be possible to exclude the FGOALS-f3-L model and to add the BCC-CSM2-MR (ECS = 3.04 °C) and MRI-ESM2-0 (ECS = 3.15 °C) models. FGOALS-f3-L may be excluded because, despite its ECS is on the border limit (3.0 °C), its TCR appears to be too high (1.94 °C). Instead, the other two models might be included since, despite having an ECS slightly > 3.0 °C, their TCR is low (1.72 °C and 1.64 °C, respectively). In fact, a low-TCR macro-GCM would have a TCR equal to or less than 1.8 °C. All the other CMIP6 GCMs should be avoided for climate-change policy since they are characterized by too high ECS or TCR values and, as an ensemble, they overestimate the warming observed from 1980 to 2022.

In any instance, the optimal selection of GCMs that must be chosen might be considered arbitrary. I propose an alternative methodology that considers all available simulations. The ensemble projections of each of the three macro-GCMs can be empirically scaled to best fit the observed warming from 1980–1990 to 2012–2022 to ensure an ideal outcome compatible with the observed warming during the same period (and add a little bit more dispersion associated with the internal variability of the models). In this study, the HadCRUT5 and UAH-MSU lt v. 6.0 temperature records are deemed representative of the surface-based and satellite-based global surface temperature estimations.

The necessary scaling factors are obtained from the median values reported in Table 2 for each of the three ECS macro-GCMs, as well as the warming of 0.605 °C and 0.432 °C shown by the HadCRUT5 and UAH-MSU lt v. 6.0 records from 2012 to 2022 relative to 1980–1990, respectively. Thus, we have:

- Case #1 uses HadCRUT5 — the Hist + SSP2-4.5 GCM simulations of the high-ECS group are scaled by the factor 0.605/0.97 = 0.62, those of the medium-ECS group are scaled by the factor 0.605/0.80 = 0.77, and those of the low-ECS group are scaled by the factor 0.605/0.620 = 0.98;
- Case #2 uses UAH-MSU lt v. 6.0 — the Hist + SSP2-4.5 GCM simulations of the high-ECS group are scaled by the factor 0.432/0.97 = 0.45, those of the medium-ECS group are scaled by the factor 0.432/0.80 = 0.54, and those of the low-ECS group are scaled by the factor 0.432/0.620 = 0.70.

The above ratios are characterized by a statistical relative error of about ± 5%.

In Case #1, the climate change projection ranges for the 21st century do not differ much from those determined only from the low-ECS macro GCM simulations mentioned in Section 4 and reported in Table 3 because the scaling factor in such a case is close to one. Case #2, on the other hand, necessitates a 30% reduction in the climate simulations of the low-ECS macro GCM. The [2.5%, 17%, 50%, 83%, 97.5%] percentiles of the simulated warming distributions at 1850–1900 covering each decade from 2000 to 2100 are shown in Table 4.

Due to the used scaling factors, the warming hindcasted by the models from 1850–1900 to 1980–1990 may not match the observed warming. This is unimportant because past data are characterized by increasing uncertainty (Morice et al., 2021). Furthermore, if surface temperature records from 1980 to 2022 must be scaled down to match the satellite-based records because of, for example, urban heat and other non-climatic contaminations, also the real warming from the pre-industrial period to the present would be less than what was reported (cf. Scafetta, 2021a; Connolly et al., 2023).

Fig. 5A's left panel depicts Case #1. It shows the estimated global temperature changes from 1980 to 2100, as well as their percentile — likely (66%) and very likely (95%) — ranges, based on the Hist + SSP2-4.5 scenario and scaling the CMIP6 GCM simulations to best hindcast the warming shown by the HadCRUT5 global surface temperature record from 1980–1990 to 2012–2022. The temperature record is baselined with the modeled hindcast mean from 1980 to 1990.

Fig. 5B's left panel depicts Case #2. It is the same as in Fig. 5A, but the CMIP6 GCM simulations are now scaled to best hindcast the warming seen in the UAH-MSU lt v. 6.0 temperature record from 1980–1990 to 2012–2022. This scenario should be used if it is demonstrated that non-climatic warm biases influence global surface temperature records and that the satellite lower troposphere temperatures (UAH-MSU or NOAA STAR) better represent the actual global surface warming from 1980 to 2022. The temperature record is baselined with the modeled hindcast mean from 1980 to 1990.

The displayed percentile ranges of the estimated global temperature changes shown in Fig. 5A and B are reported in Table 4 for each decade from 2000 to 2100. The right panels of Fig. 5 depict the burning ember diagrams (in function of the global temperature warming) of the main five global reason for concern (RFC) assuming low to no adaptation as reported in the IPCC AR6 (Pörtner et al., 2022). The five RFCs are described as:

- RFC1 (unique and threatened systems) — ecological and human systems with limited geographic ranges due to climate-related factors and high endemism or other distinguishing characteristics such as coral reefs, the Arctic and its indigenous peoples, mountain glaciers, and biodiversity hotspots;
- RFC2 (extreme weather events) — impacts and risks to human health, livelihoods, assets and ecosystems from extreme weather events such as heatwaves, heavy rain, drought and associated wildfires, and coastal flooding;
- RFC3 (distribution of impacts) — impacts and risks that disproportionately affect specific groups as a result of uneven distribution of physical climate change hazards, exposure, or vulnerability;
- RFC4 (global aggregate impacts) — impacts on socio-ecological systems that may be aggregated globally into a single metric, such as monetary damages, lives lost, species extinction, or global ecosystem deterioration;

Table 4
Percentiles [2.5%, 17%, 50%, 83%, 97.5%] of the distributions of the best estimated projected warming from 1850 to 1900 to the 11-year periods covering each decade from 2000 to 2100. The curves are depicted in Figs. 5 and 7. Modeling.

		Temperature change from 1850 to 1900 (°C)									
	Percentile	2005	2015	2025	2035	2045	2055	2065	2075	2085	2095
	97.5%	1.11	1.30	1.59	1.85	2.06	2.36	2.57	2.75	2.96	3.09
Case #1	83.0%	0.95	1.14	1.41	1.66	1.89	2.13	2.35	2.55	2.70	2.82
Fig. 5A	50.0%	0.74	0.90	1.15	1.35	1.59	1.80	1.97	2.10	2.22	2.34
(HadCRUT5)	17.0%	0.48	0.65	0.86	1.04	1.23	1.43	1.58	1.72	1.86	1.94
	2.5%	0.30	0.52	0.71	0.90	1.05	1.24	1.38	1.51	1.62	1.68
	97.5%	0.80	0.93	1.13	1.32	1.47	1.68	1.84	1.96	2.11	2.21
Case #2	83.0%	0.67	0.82	1.01	1.19	1.34	1.52	1.68	1.82	1.92	2.02
Fig. 5B	50.0%	0.53	0.64	0.82	0.96	1.13	1.29	1.41	1.50	1.59	1.67
(UAH-MSU lt v. 6.0)	17.0%	0.34	0.46	0.62	0.74	0.87	1.03	1.13	1.23	1.33	1.39
	2.5%	0.22	0.37	0.51	0.65	0.75	0.89	0.99	1.07	1.16	1.20
	97.5%	1.18	1.26	1.34	1.50	1.67	1.98	2.25	2.38	2.52	2.52
Case #3	83.0%	1.00	1.10	1.20	1.30	1.51	1.75	2.02	2.17	2.26	2.26
Fig. 7A	50.0%	0.80	0.85	0.94	1.00	1.21	1.42	1.64	1.73	1.78	1.77
(HadCRUT4.6)	17.0%	0.54	0.60	0.65	0.69	0.85	1.06	1.25	1.34	1.41	1.37
	2.5%	0.37	0.47	0.51	0.55	0.68	0.87	1.05	1.13	1.18	1.11

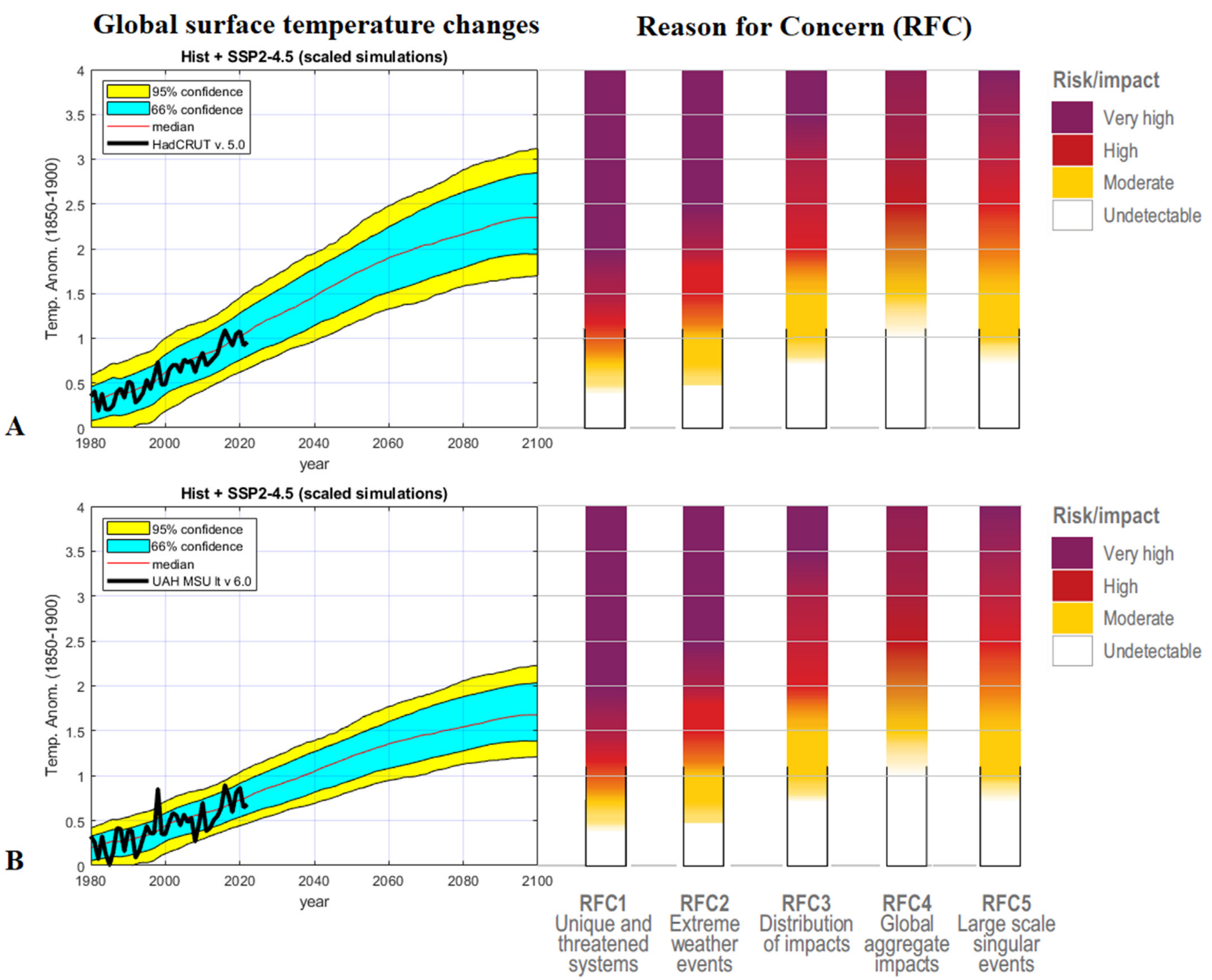

Fig. 5. (A) Estimated global temperature changes using the Hist + SSP2-4.5 scenario and scaling the CMIP6 GCM simulations to optimally hindcast the HadCRUT5 global surface temperature warming from 1980 to 1990 to 2012–2022. [(B) The same using CMIP6 GCM simulations scaled to optimally hindcast the UAH-MSU lt v. 6.0 temperature warming from 1980 to 1990 to 2012–2022. Both temperature records are baselined with the modeled hindcast mean from 1980 to 1990. Table 4 tabulates the depicted percentile ranges. [Right] Burning ember diagrams (in function of the global temperature warming) of the main five global reason for concern (RFC) assuming low to no adaptation reported by the IPCC AR6 (Pörtner et al., 2022).

- RFC5 (large-scale singular events) — relatively significant, rapid, and potentially permanent changes in systems driven by global warming, such as ice sheet collapse or thermohaline circulation slowdown.

Fig. 5A suggests that the impacts and risks of climate changes for all five RFCs can be relatively moderate (yellow-orange flag) until 2050, and they will gradually increase until 2100. Only some unique and particularly critically threatened environmental systems may be at higher risk. In fact, Table 4 shows that the very likely (95% confidence) warming should range from 1.15 °C to 2.21 °C (median 1.70 °C) by 2040–2060, and 1.65–3.03 °C (median 2.28 °C) by 2080–2100.

Fig. 5B shows the 21st-century climate projection depicted in Fig. 5A reduced by roughly 30% to fit the UAH-MSU lt temperature records: the 95% confidence warming ranges from 0.82 °C to 1.58 °C (median 1.21 °C) by 2040–2060, and from 1.18 °C to 2.16 °C (median 1.63 °C) by 2080–2100. These temperature projections are much lower than the IPCC AR6 estimates. For example, simply using the GCMs with ECS between 2.5 °C and 4.0 °C, which is the IPCC likely ECS-range, the global warming is estimated to be between 1.37–2.61 °C by 2040–2060 and 1.98–3.82 °C by 2080–2100 (Table 3).

Cases #1 and #2 imply that the realistic impacts and risks of climate change could be moderate (yellow-orange flag) in all five RFCs until 2100 also using the SSP2-4.5 scenario.

5.2. GCM scaling assuming natural oscillations

Scafetta (2010, 2013, 2021c) proposed empirical models for global climate change based on the evidence that climate records appear to be characterized by several oscillations that could be related to solar or astronomical harmonics. From a physical point of view it might be possible that cloud formation, which the GCMs partially parameterize with some free parameters that are carefully tuned (Mauritsen et al., 2019; Mignot et al., 2021), may also strongly depend on some non-radiative forcing (cosmic rays, interplanetary dust, etc.) modulated by solar magnetic activity (Shaviv, 2002; Svensmark et al., 2016; Scafetta et al., 2020; Svensmark, 2022; Scafetta, 2023c), which the state-of-the-art climate models ignore. In fact, the GCMs can also be directly tuned just to obtain an improved match to the instrumental temperature record by changing their free parameters (Mauritsen and Roeckner, 2020), which leaves the possibility of missing mechanisms (cf. Kaufman and Broadman, 2023).

The proposed model assumed that the warming indicated by global surface temperature records (e.g., HadCRUT3 and HadCRUT4) is sufficiently accurate. It is made of a multi-harmonic natural component simulating the hypothesized and empirically derived astronomical/solar effect superimposed on an empirically estimated anthropogenic-plus-volcanic effect scaled from the GCM simulations. The empirical model also includes a quasi 9.1-year oscillation that appears to be caused by solar-lunar tidal forcings. Scafetta (2010, 2012a, 2013) estimated that if such natural solar/astronomical harmonic contribution is considered, the climate's sensitivity to anthropogenic and volcanic forcings should be approximately halved. This means that the empirically determined anthropogenic-plus-volcanic effect can be approximated by multiplying the ensemble average of all GCM simulations by a factor of about 0.5. For more information, see Scafetta (2013, 2023c). The underlying hypothesis is that the harmonics that have characterized climate change in recent decades, centuries, and millennia will continue to do so also throughout the 21st century.

Fig. 6 compares the original CMIP6 GCM ensemble average simulations to the proposed empirical model. The latter is based on Scafetta (2021b)'s 13-harmonics set (representing the solar-astronomical induced variability of the climate system), which adds 7 interannual identified harmonics to Scafetta (2013)'s original six harmonics model covering the decadal-to-millennial scales. The model is completed by an empirically derived anthropogenic-plus-volcanic signal, which is obtained by halving the ensemble average of the GCM simulations, implying that the actual ECS could range between 0.9 and 2.8 °C, as recently evaluated by independent studies (Lewis, 2023; Scafetta, 2023b; Spencer and Christy, 2023).

The empirical global surface temperature model is proposed as Eq. (1)

$$T(t) = T_0 + \sum_{i=1}^{13} A_i \sin\left[2\pi(f_i \times (t-2000) + \alpha_i)\right] + 0.5 \times GCM(t) \quad (1)$$

where the coefficients A_i, f_i and α_i per i = 1, …, 13 are reported in Table 5, GCM(t) is the ensemble average of the GCM simulations for each SSP scenarios (which were downloaded from KNMI Climate Explorer), and T_0 is the reference baseline of the temperature anomalies that can be chosen, for example, to make $T_{1850-1900} = 0$ °C. The harmonic coefficients were derived from astronomical considerations and optimized for best data fitting using a Montecarlo approach (Scafetta, 2021b). Throughout the Holocene, the period of the quasi millennial cycle was theoretically and empirically estimated to be about 983 years (Scafetta, 2012b), but f_1 in Eq. (1) corresponds to a period of 760 years that was chosen to simulate the skewness of the millennial cycle, which could be modeled with the addition of the quasi 2318-year Hallstatt solar cycle (Scafetta et al., 2016; Scafetta, 2020). Indeed, paleoclimate temperature reconstructions from the last millennium typically show a minimum around 1680 (corresponding to the coldest period of the Little Ice Age during the Maunder solar minimum) and a millennial maximum around 1077; the next solar millennial grad-maximum is expected around 2060. Scafetta (2012b, Fig. 8) showed that the proposed semi-empirical model well hindcast the quasi-millennial cycle observed in climate records throughout the Holocene despite both its phase and period were deduced from solar-astronomical considerations alone. Scafetta (2012a, Fig. 5B) validated an early version of the same harmonic model by independently calibrating its decadal and multi-decadal harmonics for the years 1850–1950 and 1950–2011, demonstrating that the two independent climate hindcasts closely coincided from 1850 to 2050 and optimally reproduced the global surface temperature record from 1850 to 2011. Scafetta (2021b, figures 11 and 14) also used the proposed model to reproduce temperatures since the Medieval period, and Scafetta (2021b, figure 15) demonstrated that the model, which was calibrated using data up to 2014, could also forecast the warm periods that occurred in 2015–2016 and around 2020, as well as the approaching 2023–2024 warm period.

The left panels of Fig. 6 zoom in on the right panels between 1980 and 2030 to better show the models' performance over the last 50 years. The temperature data used here are the (infilled) HadCRUT v.5 (Morice et al., 2021), which is chosen as an average representative of the most recent global surface temperature records (Scafetta, 2023a), and the UAH-MSU lt v 6.0 global temperature record by Spencer et al. (2017), which is nearly identical to the NOAA STAR v. 5.0 lt record (Zou et al., 2023). The lower troposphere temperature records are adopted as representative of the real surface temperature change since 1980 if the surface records are influenced by non-climatic biases (Connolly et al., 2021, 2023; Scafetta, 2021a; Soon et al., 2023). Finally, the picture depicts global aggregated impact estimates based on the burning ember diagram proposed by the IPCC AR6 (Pörtner et al., 2022). The data represent temperature anomalies relative to the pre-industrial period of 1850–1900.

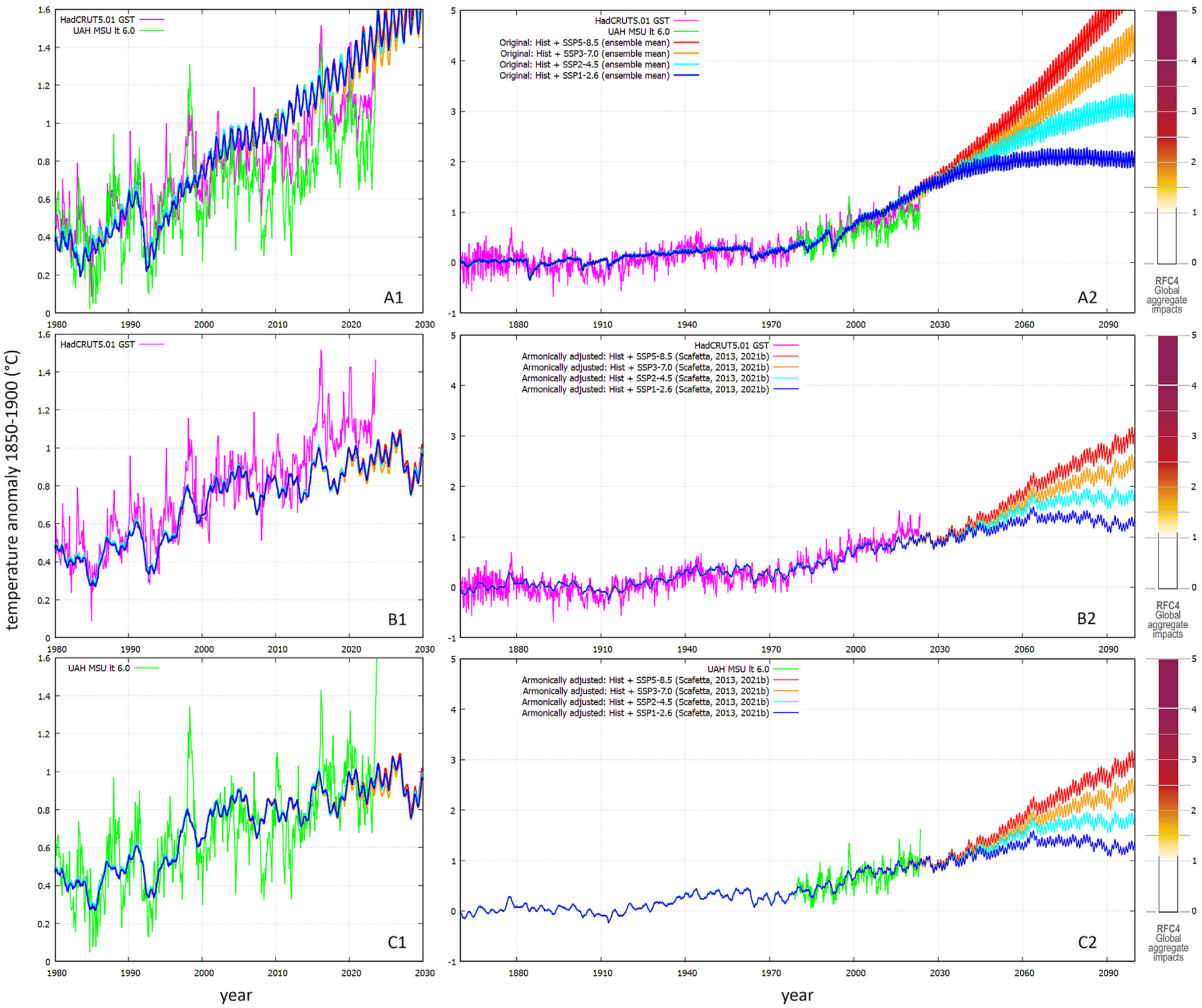

Fig. 6. Comparison of the climate simulations and projections with their relative global aggregated impacts and risks obtained with (A) the ensemble average CMIP6 GCM simulations and (B and C) the harmonic empirical global climate models proposed by Scafetta (2010, 2013, 2021b). The temperature data used are the (infilled) HadCRUT v.5 (Morice et al., 2021) and the UAH-MSU lt v. 6.0 lower troposphere global temperature records (Spencer et al., 2017).

Table 5
Coefficients for the harmonic component of the empirical climate model given by Eq. (1).

i	A_i (°C)	*fi* (1/y)	α_i
1	0.3228	0.001318	0.171
2	0.05843	0.008696	0.424
3	0.08583	0.01639	0.152
4	0.03339	0.0500	0.148
5	0.02407	0.09615	0.02
6	0.02651	0.1075	0.497
7	0.02163	0.1340	0.711
8	0.02721	0.1666	0.617
9	0.02598	0.1909	0.409
10	0.03257	0.2086	0.931
11	0.02758	0.2752	0.767
12	0.02537	0.2812	0.792
13	0.02472	0.3480	0.975

Fig. 6A depicts the original GCM ensemble mean simulations. Only the net-zero emission SSP1-2.6 scenario ensures that global surface temperatures do not significantly exceed the 2 °C (safe) threshold (Gao et al., 2017; Tol, 2015), which satisfies to the Paris Agreement warming targets. However, as shown in 6-A1, these average models are running too hot in relation to both global surface and lower troposphere temperature records.

Fig. 6B compares the four SSP average simulations generated by the proposed empirical model of Eq. (1) to the HadCRUT5 record. The figure shows that, in addition to the (net-zero emission) SSP1-2.6 scenario, also the moderate SSP2-4.5 scenario would ensure a global surface temperature of less than 2 °C throughout the 21st century, with an average of about 1.8 °C by 2080–2100. Furthermore, the extreme (and highly unlikely) SSP5-8.5 scenario is projected to warm the global climate on average by only 3 °C relative to pre-industrial levels, which is only moderately concerning. However, as illustrated in 6-B1, the empirical model appears to underestimate the HadCRUT5-measured global surface temperature warming. Yet, it agrees well with the HadCRUT3 and HadCRUT4 records (Scafetta, 2013, 2021b); therefore, the current discrepancy with the (infilled) HadCRUT5 appears to be attributa-

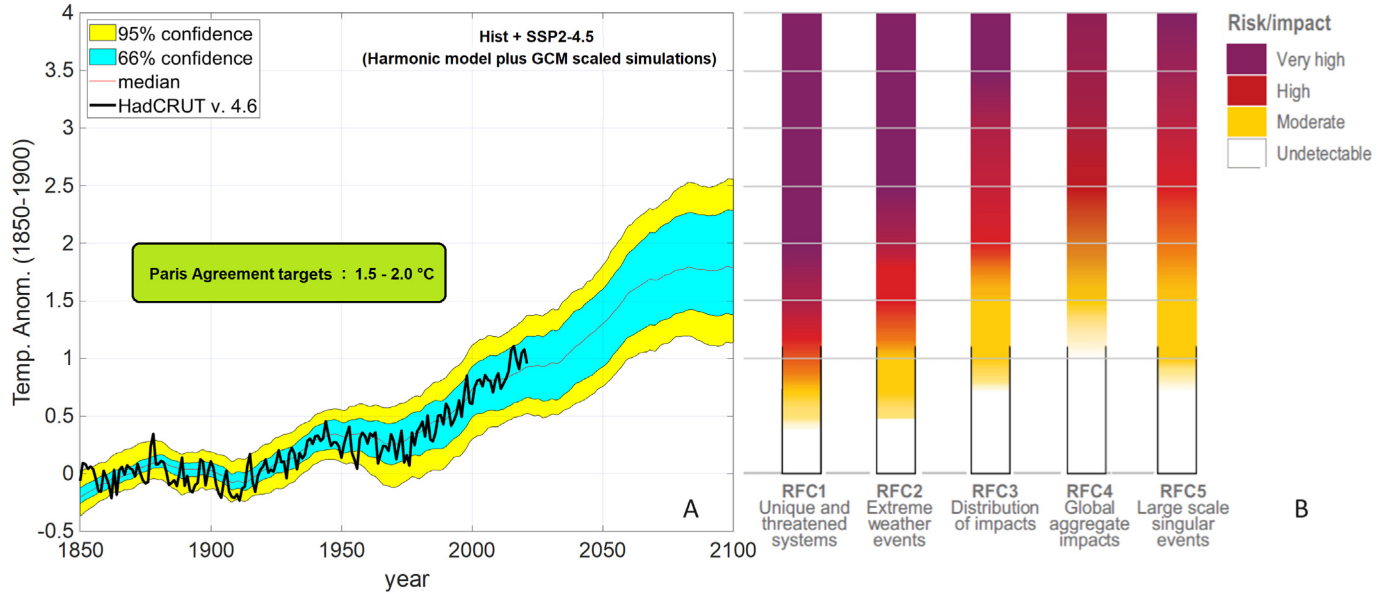

Fig. 7. (A) The harmonic empirical global climate model with the SSP2-4.5 scenario, against the HadCRUT4.6 record (1850–2021) (Morice et al., 2012). (B) Burning ember diagrams (in function of the global temperature warming) of the main five global reason for concern (RFC) assuming low to no adaptation reported by the IPCC AR6 (Pörtner et al., 2022). Table 4 tabulates the depicted percentile ranges from 2000 to 2100.

ble to the adjustments made to the latter, which concealed the 2000–2014 temperature "hiatus" or "pause" that is still revealed by the satellite temperature records.

In fact, Fig. 6C is like Fig. 6B, except my model simulations are now compared to the lower troposphere temperature record from UAH-MSU. The empirical model (first proposed by Scafetta, 2010, 2013) appears to have accurately predicted the observed warming. As a result, if satellite temperature data better represent the actual global surface warming from 1980 to 2022, the model's empirical calibration can be assumed validated, potentially making its future climate projections trustworthy as well.

Fig. 7A compares the harmonic empirical global climate model with the SSP2-4.5 scenario to the HadCRUT4.6 record (Morice et al., 2012), which is used here as a compromise between the (infilled) HadCRUT5 and the lower troposphere satellite temperature records. Scafetta (2021b) calibrated his empirical model until 2014 using the HadCRUT4.6 record. The model projection range is equivalent to Fig. 5A. Fig. 7A also shows that the proposed harmonic empirical model reconstructs the multidecadal modulation (consisting of quasi 60-year oscillations forming a sequence of quasi-30-year warming or cooling periods) observed in the temperature record since 1850 much better than the GCM simulations, which show only monotonically increasing patterns interrupted by sporadic volcano eruptions (see Figs. 1 and 6A2); the same quasi-60-year modulation can be reconstructed with appropriate total solar activity records, as demonstrated by Scafetta (2023c).

By extending the same natural modulation up to 2080–2100, the empirical climate projection predicts that the temperature will range from 1.15 °C to 2.52 °C (median 1.78 °C), which roughly matches the 1.26–2.82 °C range produced by the SSP1-2.6 scenario using GCMs with ECS ranging from 2.5 °C to 4.5 °C as reported by the IPCC. Table 4 reports the depicted percentile ranges from 2000 to 2100.

The warming rate is expected to remain relatively low from 2000 to 2035 and from 2065 to the end of the century because the empirical model predicts negative phases of the Atlantic Multidecadal Oscillation (AMO) during these periods, whereas the warming rate is expected to increase from 2035 to 2065 when the AMO is forecasted to be positive. The AMO highlights a well-known large quasi-60-year oscillation of the climate system that is not predicted by GCMs (Scafetta, 2013) but has been observed for millennia (Knudsen et al., 2011; Wyatt and Curry, 2013; Scafetta, 2014a); it is most likely of solar/astronomical origin, along with other larger oscillations of the climate system (Neff et al., 2001; Scafetta et al., 2013; Scafetta, 2014b, 2020, 2023c; Scafetta et al., 2020).

6. Summary of the results

Figs. 5 and 7 show three "realistic" global warming projections for the 21st century. They imply that the impacts and risks of realistic climatic changes are significantly more moderate than what the IPCC expected.

The left panels of Fig. 8 summarize the estimated warming in 2040–2060 and 2080–2100 according to the SSP2-4.5 scenario and the warming projected ranges at 67% and 95% confidence as deduced in four cases (see Tables 3 and 4):

Ranges #O are the original ones and derive from the GCMs with ECS values between 2.5 °C and 4 °C, which are in line with the IPCC's prediction of its likely ECS range;

Ranges #1 derive from the GCMs scaled on the low-ECS macro GCM and assumes the 1980–2022 warming of the HadCRUT5 record, as shown in Fig. 5A;

Ranges #2 derive from the GCMs scaled on the low-ECS macro GCM and assumes the 1980–2022 warming of the UAH-MSU LT v. 6.0 record, as shown in Fig. 5B.

Ranges #3 derive from the empirical harmonic model (Eq. 1) depicted in Fig. 7A.

The right panels of Fig. 8 show a selection of the same burning ember diagrams (in function of the global temperature warming) of regional and global risk assessments relative to several ecosystems, and disease-health situations adopted by the IPCC AR6. A detailed explanation of each RFC is found in Pörtner et al. (2022). The first line represents examples of ecosystem risk assessments; the second line represents examples of climate sensitive health

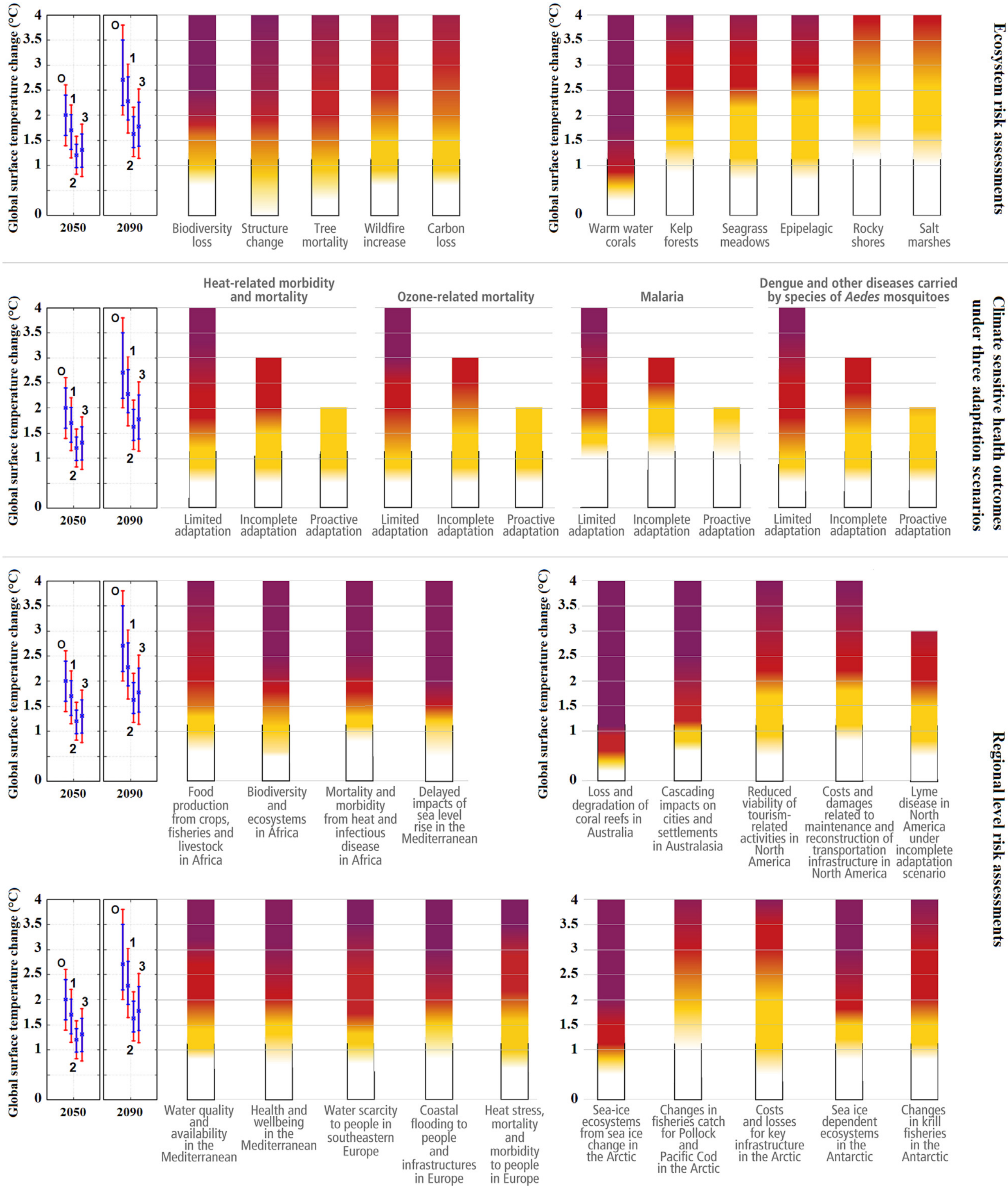

Fig. 8. [Left] Estimated warming in 2040–2060 and 2080–2100 according to the SSP2-4.5 scenario and three cases: (O-original) using the GCMs with ECS between 2.5 °C and 4 °C (IPCC option); (1) using the GCMs scaled on the low-ECS macro GCM and the HadCRUT5 record (Fig. 5A); (2) using the GCMs scaled on the low-ECS macro GCM and the UAH-MSU lt v. 6.0 record (Fig. 5B); (3) using the empirical harmonic model (Eq. (1) and the HadCRUT4.6 record (Fig. 7A). [Right] Burning ember diagrams (in function of the global temperature warming) representing the estimated global and local impacts and risks of global warming for several ecosystems and health outcomes as reported in the IPCC AR6 (Pörtner et al., 2022, Summary for Policymakers).

outcomes under limited, incomplete, and proactive adaptation scenarios; the third and fourth lines represents examples of regional level risk assessments. Unless otherwise specified, the burning ember diagrams represent situations in which little or no adaptation is planned. As more sophisticated adaptation policies are implemented, the color scale shifts upward in a way like what is shown in the second row of Fig. 8.

Most of the time, for cases #1–3, the impacts and risks of climate changes would be moderate (yellow-orange flag) until 2050. The SSP2-4.5 scenario may also ensure an average global surface temperature of less than 2 °C by 2100, and hence also this moderate SSP should be considered compatible with the Paris Agreement warming objective. As a result, while suitable adaptation techniques may always be required, they may be rather affordable because the impacts and risks of actual future climate change are expected to be non alarming.

7. Discussion and conclusion

The IPCC used the CMIP6 GCMs to assess the probable risks and impacts of climate change on global and regional scales over the next century (Masson-Delmotte et al., 2021; Pörtner et al., 2022). Climate change estimates are influenced by the climate's sensitivity to radiative forcing as well as by the projected greenhouse gas emissions, which are linked to varying rates and kinds of socioeconomic developments. However, there is a great deal of uncertainty in both conditions that must be restricted to properly assessing realistic climate-change impacts and risks for the 21st century and developing appropriate climate policies to optimally address them.

The ECS of the CMIP6 GCMs ranges between 1.8 °C and 5.7 °C, but the IPCC AR6 acknowledged the existence of a "hot" model problem and claimed that the actual ECS may likely range between 2.5 °C and 4.0 °C, with a best estimate of around 3.0 °C (Sherwood et al., 2020; Hausfather et al., 2022). However, recent research suggests that the expected ECS range should vary within lower values between 1.5 °C and 3 °C (Nijsse et al., 2020; Scafetta, 2022, 2023a, b; Lewis, 2023; Spencer and Christy, 2023). Furthermore, according to a number of empirical studies, the actual ECS values could even be significantly lower, ranging between 1 °C and 2 °C (Lindzen and Choi, 2011; Scafetta, 2013, 2023c; Bates, 2016; McKitrick and Christy, 2020; Stefani, 2021).

The IPCC AR6 investigates a range of SSP scenarios for the 21st century without assigning a probability to their plausibility. In any case, despite the questionable visibility given to SSP5-8.5 (the worst-case scenario), which yields the largest and most alarming projected global warming of up to 4–8 °C (66%) by 2080–2100, table 12.12 of the IPCC AR6 (Masson-Delmotte et al., 2021, p. 1856) already reports for the entire 21st century low confidence in the direction of any change in the frequency, severity or extent of frost, river floods, landslides, aridity, hydrological drought, agricultural and ecological drought, fire weather, mean wind speed, severe wind storms, tropical cyclones, sand and dust storms, heavy snowfall and ice storms, hail, snow avalanche, coastal floods, coastal erosion, marine heatwaves, air pollution weather or radiation at earth's surface. Medium and high confidence of changes are mostly expected in climatic impact-driver types more directly associated with increasing atmospheric CO_2 concentration at surface and global warming such as increasing mean air temperature, extreme heat, sea level, mean ocean temperature, ocean salinity and ocean acidity; with decreasing cold spell, snow, glacier and ice sheet, permafrost, lake, river and sea ice, and dissolved oxygen; mean precipitation will increase in some regions and decrease in others.

However, recent research argued that the alarmistic SSP3-7.0 and SSP5-8.5 scenarios are likely and very likely unrealistic, respectively (Burgess et al., 2020; Hausfather and Peters, 2020; Pielke and Ritchie, 2021a,b). These studies indicate that the radiative forcing functions derived from the SSP2-4.5 (or even SSP2-3.4) scenario are the most plausible. The SSP2-4.5 is a moderate scenario; it projects about half of the 21st-century warming than what the SSP5-8.5 scenario does (Fig. 1) and is thus far less alarming.

With the aforementioned factors in mind, it was proposed here to use only the SSP2-4.5 scenario and the GCMs with ECS $\leq$ 3 °C to more precisely assess "realistic" global and regional impacts and risks that could be associated with climate changes that are expected to occur in the 21st century, and to compare them with the Paris Agreement warming target of keeping global surface temperature < 2 °C above the pre-industrial levels throughout the 21st century. To optimize the result even more, the simulation ensembles containing the low, medium, and high-ECS macro-GCMs were linearly scaled to best reflect the real global surface warming recorded from 1980–1990 to 2012–2022.

According to the IPCC, if there is little-to-no adaptation, the impacts and risks of projected climate change will be moderate-high (orange-red flag) by 2040–2060, and the situation might worsen considerably by 2100 even if the SSP2-4.5 moderate scenario is implemented. In fact, according to the analysis reported in Table 3, the GCMs within the IPCC's preferred ECS range of 2.5–4.0 °C project a warming of 1.98–3.82 °C by 2080–2100. Thus, the IPCC (Masson-Delmotte et al., 2018) analysis suggests that only net-zero-emission scenarios like the SSP1-2.6 (which could produce a warming of 1.26–2.82 °C by 2080–2100) should be adopted to avoid too dangerous climatic changes, which are expected to begin if global surface temperatures rise more than 2–2.5 °C above the 1850–1900 level in a few decades (Gao et al., 2017; Tol, 2015). Climate-change alarmism and world-wide proposals for prompt implementations of net-zero emission policies are only based on such claims.

However, using only the low-ECS models (ECS $\leq$ 3.0 °C) and the SSP2-4.5 scenario, Table 3 suggests that global warming in the 21st century will be moderate, ranging from 1.36 °C to 2.25 °C (median 1.77 °C) by 2050 and from 1.96 °C to 2.83 °C (median 2.28 °C) by 2080–2100, which partially overlaps with the upper warmer half of the climate projection obtained using the SSP1-2.6 scenario and the GCMs with ECS of 2.5–4.0 °C. Thus, climate change impacts and risks will worsen by the end of the 21st-century, albeit at a slower rate than predicted by the IPCC using the same SSP2-4.5 scenario. As a result, the SSP2-4.5 scenario, which is moderate and affordable, may be close enough to roughly meet the Paris Agreement warming target, whereas the SSP2-3.4 scenario, which could be even more realistic (Pielke et al., 2022), should even more likely fully meet it.

I also proposed an alternative methodology for estimating "realistic" 21st-century climate projections and assessing their respective impacts and risks. In fact, the low-ECS macro-GCM appears to be slightly warmer than global surface temperature records and there are serious concerns about the reliability of the global surface temperature records, which cannot be ignored. In fact, their warming appears to be excessive in comparison to alternative temperature records, such as satellite-based ones relative to the lower troposphere (Spencer et al., 2017; Zou et al., 2023), and there are various evidences suggesting their contamination from urban heat islands and other non-climatic surface factors (Connolly et al., 2021; Scafetta, 2021a, 2023b; Soon et al., 2023; Spencer, 2023). There are also concerns regarding the ability of the GCMs to properly reconstruct decadal to millennial natural climate oscillations (e.g.: Scafetta, 2013, 2021b, 2023c). As a result, all GCMs may be grossly inadequate for estimating climate change in the 21st century, as also McKitrick and Christy (2020) concluded. Thus, the models likely need to be corrected and upgraded with new relevant physical mechanisms. It is possible to agree with McCarthy and Caesar (2023) who recently showed the inability of the CMIP5 and CMIP6 GCMs in properly hindcasting the Atlantic Meridional Overturning Circulation and concluded "if these models cannot reproduce past variations, why should we be so confident about their ability to predict the future?".

To address the above issues, I have proposed an alternative methodology that uses empirical modifications of the actual GCM projection ensembles via appropriate linear scaling in such a way to simulate the outputs of hypothetical climate models that could accurately represent the warming observed from 1980 to 2022.

The 1980–2022 period was selected because it is covered by a variety of temperature records with low statistical errors. This methodology would essentially simulate hypothetical GCMs that are supposed to optimally reproduce the data. Simple testing validates the proposed methodology because scaling the projection ensembles of the three macro-GCMs to a similar level from 1080–1990 to 2011–2022 results in projection ensembles that approximately overlap throughout the 21st century.

The proposed methodology may also be justified by considering that the GCMs are extremely sensitive to small modifications of their internal free parameters, in particular to those regarding cloud formation, and even GCM modelers adopt complex tuning approaches to explicitly calibrating them to better match historical data (Mauritsen and Roeckner, 2020; Mignot et al., 2021). Section 4 proposes and investigates several of these modeling approaches, the results of which are depicted in Figs. 5 and 7.

If the warming of the HadCRUT5 record from 1980 to 1990–2011–2022 is assumed correct, it is found that the SSP2-4.5 scenario produces climate projections similar to those produced by the low-ECS macro-GCM. In fact, the projected warming ranged from 1.65 °C to 3.03 °C by 2080–2100, with a median of 2.28 °C (Table 4, case #1). This conclusion is unsurprising given that the low-ECS macro-GCM has already successfully recreated the HadCRUT5 warming.

However, if the reference warming is that reported by lower troposphere satellite temperature data (Spencer et al., 2017; Zou et al., 2023), the warming of the low-ECS macro-GCM simulations must be lowered by about 30%. As a result, global warming by 2080–2100 is projected to range from 1.18 °C to 2.16 °C (median 1.63 °C) above pre-industrial levels using the SSP2-4.5 scenario (Table 4, case #2), which is well below the (safe) threshold of 2.0 °C and is even cooler than the 1.26–2.82 °C estimate obtained with the GCMs with ECS within the IPCC likely range of 2.5 °C and 4.0 °C using the SSP1-2.6 net-zero emission scenario.

A similar result was obtained with an empirical climate model that assumes that the global surface temperature record is sufficiently accurate, but also takes into account temperature changes caused by empirically identified large climate cycles and/or solar effects that the CMIP6 GCMs do not replicate (Scafetta, 2010, 2013, 2021b); this case projects a warming ranging from 1.15 °C to 2.52 °C with median 1.78 °C by 2080–2100 (Table 4, case #3). Unfortunately, the IPCC ignores such semi-empirical modeling of the climate system although it has been developed and discussed in the scientific literature, and it should not be dismissed lightly given that the GCMs fail to reproduce the natural oscillations observed throughout the Holocene. They do not, for example, reproduce any of the Holocene warm periods, such as the Roman and Medieval warm periods, which indicate a quasi-millennial oscillation, a quasi-60-year oscillation, and many other natural climate oscillations. Also this kind of empirical modeling predicts very modest ECS values, ranging at least between 1 and 3 °C, but more likely between 1 °C and 2 °C (Lindzen and Choi, 2011; Scafetta, 2013, 2021b, 2023c; Bates, 2016; Stefani, 2021).

In conclusion, as Hausfather and Peters (2020) pointed out, it is past time to stop treating the worst-case climate change scenarios (e.g., SSP3-7.0 and SSP5-8.5) as the most likely outcomes, because only realistic and pragmatic scenarios, such as SSP2-4.5 or SSP2-3.4, can lead to sound policies that can be accepted by all nations. Furthermore, net-zero scenarios such as SSP1-2.6 look to be equally unattainable, as the depletion of crucial metals required for low-carbon solar and wind technologies, as well as electric vehicles and their chargers, appears to make low-carbon technology production impossible on the very large scale required to substitute fossil fuels (Groves et al., 2023). In fact, despite the IPCC AR6 reports are rather alarming because global surface temperatures were projected to rise by up to 4–8 °C above pre-industrial levels according to unrealistic shared socioeconomic pathways (see Fig. 1 and Masson-Delmotte et al., 2021), with catastrophic conse-

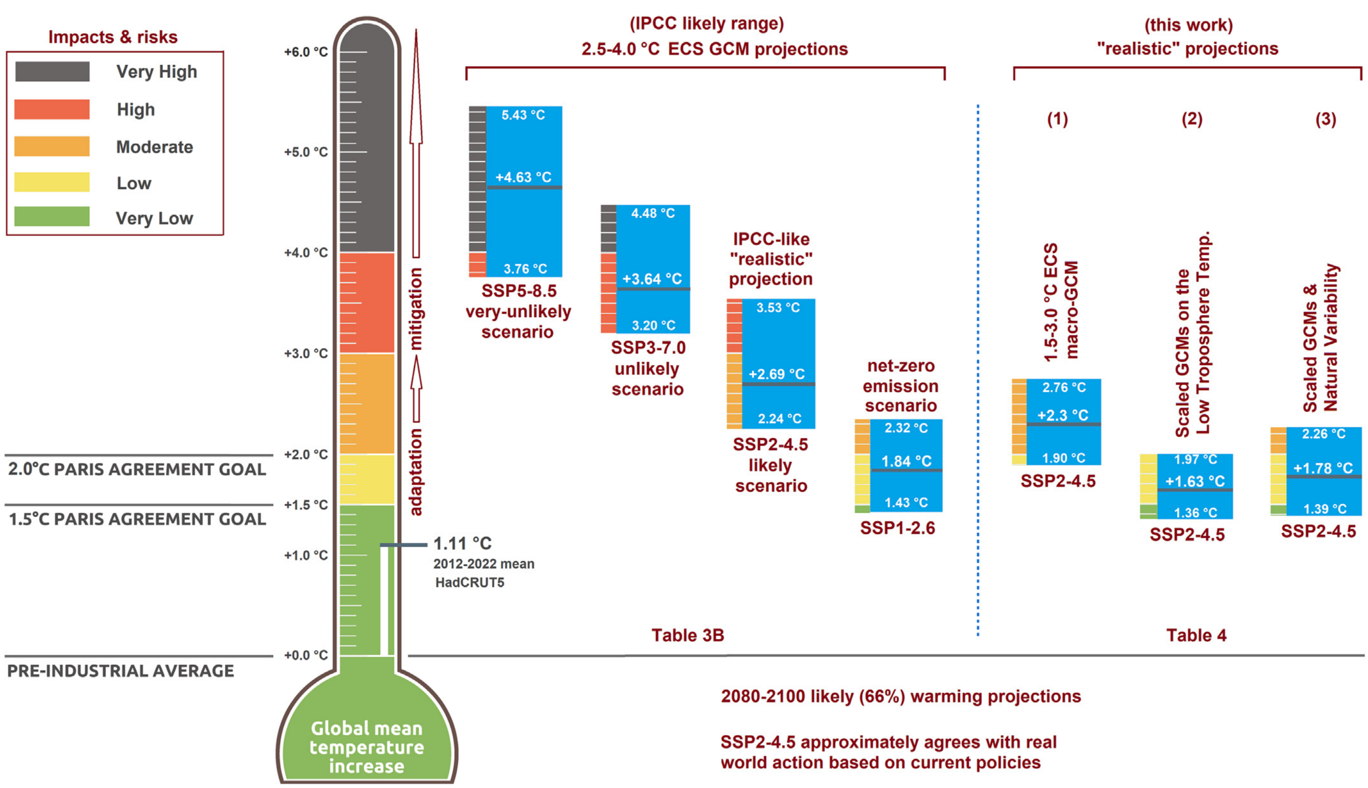

Fig. 9. Summary and comparison of the impacts and risks of global warming projections for the 2080–2100 period herein obtained (Tables 3B and 4) versus the climate "thermometer" proposed by European Commission, 2023.

quences in many situations (Pörtner et al., 2022), Figs. 5, 7 and 8 show that "realistic" climate change impacts and risks for the 21st century will likely be much more moderate than what the IPCC claims. This is because there is a growing body of evidence that the actual ECS may be rather low (1.5–3.0 °C, or even 1–2 °C) for a variety of reasons derived from direct CMIP6 GCM assessments, likely warming biases affecting global surface temperature records, and a (likely solar induced) natural variability that the current climate models do not reproduce. According to the semi-empirical climate modeling proposed above, the climate system will likely warm by less than 2.0–2.5 °C by 2080–2100, and on average less than 2.0 °C, also if the moderate SSP2-4.5 scenario is implemented. As a result, rapid decarbonization and net-zero emission scenarios such as the SSP1-2.6 are shown to be unnecessary to maintain global surface temperature < 2 °C throughout the 21st century.

Fig. 9 employs the climate "thermometer" proposed by Climate Action Tracker (2022) to summarize the above findings by contrasting the projections derived from the IPCC climate assumptions, where only the SSP1-2.6 net-zero emission scenario could satisfy the 2.0 °C target, with the new proposed assessments of "realistic" global warming impacts and risks obtained using the three semi-empirical models discussed above with the pragmatic SSP2-4.5 scenario that approximately agrees with the real world action based on current policies (Tables 3B and 4).

As a result, despite predictions that the climate system would continue to warm throughout the 21st century, there is no compelling evidence of an impending global disaster caused by man-made greenhouse gas emissions. The 2.0 °C Paris-agreement warming target for the 21st century can likely be met even under the feasible and moderate SSP2-4.5 emission scenario because future climate change is expected to be modest enough that any potential related hazards can be addressed efficiently through effective and low-cost adaptation strategies, without the need for implementing rapid, expensive, and technologically likely impossible net-zero decarbonization policies.

Data availability

The data used in the paper can be downloaded from (accessed on 01/10/2023):

- KNMI Climate Explorer: https://climexp.knmi.nl/selectfield_cmip6.cgi
- Supplementary data from Hausfather et al. (2022)
- CRUTEM5 Global Temperature: https://www.metoffice.gov.uk/hadobs/crutem5/
- CRUTEM4 Global Temperature: https://www.metoffice.gov.uk/hadobs/crutem5/
- UAH MSU v. 6.0 Global Temperature: http://vortex.nsstc.uah.edu/data/msu/v6.0/tlt/uahncdc_lt_6.0.txt

CRediT authorship contribution statement

Nicola Scafetta: Conceptualization, Formal analysis, Methodology, Writing – review & editing, Writing – original draft.

Declaration of competing interest

The author declares that he has no known competing financial interests or personal relationships that could have appeared to influence the work reported in this paper.

Appendix A. Supplementary data

The supplementary data file contains the temperature simulations depicted in Figs. 1, 5, 6 and 7. Supplementary data to this article can be found online at https://doi.org/10.1016/j.gsf.2023.101774.

References

Alley, R.B., 2000. The Younger Dryas cold interval as viewed from central Greenland. Quat. Sci. Rev. 19, 213–226.
Arrenius, S., 1896. On the influence of carbonic acid in the air upon the temperature of the ground. London, Edinburgh, and Dublin Philosophical Magazine and Journal of Science 41, 237–275.
Arrenius, S., 1906. Die vermutliche ursache der klimaschwankungen (the probable cause of climate fluctuations). Meddelanden Fran k. Vetenskapsakademiens Nobelinstitut 1, 1–10.
Atwoli, L., Baqui, A.H., Benfield, T., Bosurgi, R., Godlee, F., Hancocks, S., Horton, R., Laybourn-Langton, L., Monteiro, C.A., Norman, I., Patrick, K., Praities, N., Olde Rikkert, M.G.M., Rubin, E.J., Sahni, P., Smith, R., Talley, N., Turale, S., Vàzquez, D., 2021. Call for Emergency Action to Limit Global Temperature Increases, Restore Biodiversity, and Protect Health. N. Engl. J. Med. 385, 1134–1137.
Bates, J.R., 2016. Estimating climate sensitivity using two-zone energy balance models. Earth Space Sci. 3, 207–225.
Bond, G., Kromer, B., Beer, J., Muscheler, R., Evans, M.N., Showers, W., Hoffmann, S., Lotti-Bond, R., Hajdas, I., Bonani, G., 2001. Persistent solar influence on north atlantic climate during the holocene. Science 294 (5549), 2130–2136.
Büntgen, U., Allen, K., Anchukaitis, K.J., Arseneault, D., Boucher, É., Bräuning, A., Chatterjee, S., Cherubini, P., Churakova, O.V., Corona, C., Gennaretti, F., Grießinger, J., Guillet, S., Guiot, J., Gunnarson, B., Helama, S., Hochreuther, P., Hughes, M.K., Huybers, P., Kirdyanov, A.V., Krusic, P.J., Ludescher, J., Meier, W.-J.-H., Myglan, V.S., Nicolussi, K., Oppenheimer, C., Reinig, F., Salzer, M.W., Seftigen, K., Stine, A.R., Stoffel, M., George, S.S., Tejedor, E., Trevino, A., Trouet, V., Wang, J., Wilson, R., Yang, B., Xu, G., Esper, J., 2021. The influence of decision-making in tree ring-based climate reconstructions. Nat. Commun. 12, (1) 3411.
Burgess, M.G., Ritchie, J., Shapland, J., Pielke, R., 2020. IPCC baseline scenarios have over-projected CO_2 emissions and economic growth. Environ. Res. Lett. 16, (1) 014016.
Burgess, M.G., Becker, S.L., Langendorf, R.E., Fredston, A., Brooks, C.M., 2023. Climate change scenarios in fisheries and aquatic conservation research. ICES J. Mar. Sci. 80, 1163–1178.
Charney, J.G., Arakawa, A., Baker, D.J., Bolin, B., Dickinson, R.E., Goody, R.M., Leith, C. E., Stommel, H.M., Wunsch, C.I., 1979. Carbon Dioxide and Climate: A Scientific Assessment. National Research Council. Washington, DC: The National Academies Press. doi: 10.17226/12181.
Chavez, E., de Pater, I., Redwing, E., Molter, E.M., Roman, M.T., Zorzi, A., Alvarez, C., Campbell, R., de Kleer, K., Hueso, R., Wong, M.H., Gates, E., Lynam, P.D., Davies, A.G., Aycock, J., Mcilroy, J., Pelletier, J., Ridenour, A., Stickel, T., 2023. Evolution of Neptune at near-infrared wavelengths from 1994 through 2022. Icarus 404, 115667.
Christiansen, B., Ljungqvist, F.C., 2012. The extra-tropical Northern Hemisphere temperature in the last two millennia: Reconstructions of low-frequency variability. Clim. Past 8, 765–786.
Climate Action Tracker, 2022. The CAT Thermometer. https://climateactiontracker.org/global/cat-thermometer/ (access November 2022).
Connolly, R., Soon, W., Connolly, M., Baliunas, S., Berglund, J., Butler, C.J., Cionco, R. G., Elias, A.G., Fedorov, V.M., Harde, H., Henry, G.W., Hoyt, D.V., Humlum, O., Legates, D.R., Lüning, S., Scafetta, N., Solheim, J.-E., Szarka, L., van Loon, H., Herrera, V.M.V., Willson, R.C., Yan, H., Zhang, W., 2021. How much has the sun influenced northern hemisphere temperature trends? an ongoing debate. Res. Astron. Astrophys. 21 (6), 131.
Connolly, R., Soon, W., Connolly, M., Baliunas, S., Berglund, J., Butler, C.J., Cionco, R. G., Elias, A.G., Fedorov, V.M., Harde, H., Henry, G.W., Hoyt, D.V., Humlum, O., Legates, D.R., Scafetta, N., Solheim, J.-E., Szarka, L., Herrera, V.M.V., Yan, H., Zhang, W., 2023. Challenges in the detection and attribution of Northern Hemisphere surface temperature trends since 1850. Res. Astron. Astrophys. 23, 105015.
Crippa, M., Guizzardi, D., Pagani, F., Banja, M., Muntean, M., Schaaf, E., Becker, W., Monforti-Ferrario, F., Quadrelli, R., Risquez Martin, A., Taghavi-Moharamli, P., Köykkä, J., Grassi, G., Rossi, S., Brandao De Melo, J., Oom, D., Branco, A., San-Miguel, J., Vignati, E., 2023. GHG emissions of all world countries. Publications Office of the European Union, Luxembourg. https://edgar.jrc.ec.europa.eu/report_2023.
Czymzik, M., Muscheler, R., Brauer, A., 2016. Solar modulation of flood frequency in central Europe during spring and summer on interannual to multi-centennial timescales. Clim. Past 12 (799–805), 2016.
Eddy, J.A., 1976. The Maunder Minimum. Science 192, 1189–1202.
Egorova, T., Schmutz, W., Rozanov, E., Shapiro, A.I., Usoskin, I., Beer, J., Tagirov, R.V., Peter, T., 2018. Revised historical solar irradiance forcing. A & A 615, A85.
Eyring, V., Bony, S., Meehl, G.A., Senior, C.A., Stevens, B., Stouffer, R.J., Taylor, K.E., 2016. Overview of the coupled model intercomparison project phase 6 (CMIP6) experimental design and organization. Geosci. Model Dev. 9 (5), 1937–1958.

European Commission, 2023. Climate Action, 2050 long-term strategy. https://climate.ec.europa.eu/eu-action/climate-strategies-targets/2050-long-term-strategy_en. (access December 7 2023).

Filippelli, G., Beal, L., Rajaram, H., AghaKouchak, A., Balikhin, M. A., Destouni, G., East, A., Faccenna, C., Florindo, F., Frost, C., Griffies, S., Huber11, M., Lugaz, N., Manighetti, I, Montesi, L., Pirenne, B., Raymond, P., Salous, S., Schildgen, T., Trumbore, S., Wysession, M., Xenopoulos, M., Zhang, M., 2021. Geoscientists, who have documented the rapid and accelerating climate crisis for decades, are now pleading for immediate collective action. Geophysical Research Letters, 48, e2021GL096644.

Gao, Y., Gao, X., Zhang, X., 2017. The 2 °C Global Temperature Target and the Evolution of the Long-Term Goal of Addressing Climate Change—From the United Nations Framework Convention on Climate Change to the Paris Agreement. Engineering 3, 272–278.

Ge, Q.S., Liu, H.L., Ma, X., Zheng, J.Y., Hao, Z.X., 2017. Characteristics of temperature change in China over the last 2000 years and spatial patterns of dryness/wetness during cold and warm periods. Adv. Atmos. Sci. 34, 941–951.

GEM, 2023. Global energy monitor: global coal plant tracker. Accessed on December 7, 2023. https://globalenergymonitor.org/projects/global-coal-plant-tracker/tracker/.

Groves, D.I., Santosh, M., Zhang, L., 2023. Net Zero climate remediations and potential terminal depletion of global critical metal resources: A synoptic geological perspective. Geosystems and Geoenvironment 2, (1) 100136.

Hausfather, Z., Marvel, K., Schmidt, G.A., Nielsen-Gammon, J.W., Zelinka, M., 2022. Climate simulations: recognize the 'hot model' problem. Nature 605 (7908), 26–29.

Hausfather, Z., Moore, F.C., 2022. Net-zero commitments could limit warming to below 2 °C. Nature 604, 247–248.

Hausfather, Z., Peters, G.P., 2020. Emissions – the 'business as usual' story is misleading. Nature 577 (7792), 618–620.

Hersbach, H., Bell, B., Berrisford, P., Hirahara, S., Horányi, A., Muñoz-Sabater, J., Nicolas, J., Peubey, C., Radu, R., Schepers, D., Simmons, A., Soci, C., Abdalla, S., Abellan, X., Balsamo, G., Bechtold, P., Biavati, G., Bidlot, J., Bonavita, M., Chiara, G., Dahlgren, P., Dee, D., Diamantakis, M., Dragani, R., Flemming, J., Forbes, R., Fuentes, M., Geer, A., Haimberger, L., Healy, S., Hogan, R.J., Hólm, E., Janisková, M., Keeley, S., Laloyaux, P., Lopez, P., Lupu, C., Radnoti, G., Rosnay, P., Rozum, I., Vamborg, F., Villaume, S., Thépaut, J.-N., 2020. The ERA5 global reanalysis. Q. J. R. Meteorolog. Soc. 146 (730), 1999–2049.

Hoyt, D.V., Schatten, K.H., 1993. A discussion of plausible solar irradiance variations, 1700–1992. J. Geophys. Res. Space Phys. 98 (A11), 18895–18906.

IEA, 2020: World Energy Outlook 2020. International Energy Agency (IEA), Paris, France, https://www.iea.org/reports/world-energy-outlook-2020.

IEA, 2021: World Energy Outlook 2021. International Energy Agency (IEA), Paris, France, https://www.iea.org/reports/world-energy-outlook-2021.

Ishihara, K., 2006. Calculation of global surface temperature anomalies with cobe-sst. Weather Service Bulletin 73, S19–S25.

Katata, G., Connolly, R., O'Neill, P., 2023. Evidence of Urban Blending in Homogenized Temperature Records in Japan and in the United States: Implications for the Reliability of Global Land Surface Air Temperature Data. J. Appl. Meteorol. Climatol. 62, 1095–1114.

Kaufman, D.S., Broadman, E., 2023. Revisiting the Holocene global temperature conundrum. Nature 614, 425–435.

Kerr, R.A., 2001. A variable sun paces millennial climate. Science 294 (5546), 1431–1433.

Kirkby, J., 2007. Cosmic rays and climate. Surv. Geophys. 28 (5–6), 333–375.

Knudsen, M., Seidenkrantz, M.S., Jacobsen, B., Kuijpers, A., 2011. Tracking the Atlantic Multidecadal Oscillation through the last 8,000 years. Nature Commun. 2, 178.

Knutti, R., Rugenstein, M., Hegerl, G., 2017. Beyond equilibrium climate sensitivity. Nat. Geosci. 10, 727–736.

Kutschera, W., Patzelt, G., Steier, P., Wild, E.M., 2017. The tyrolean iceman and his glacial environment during the holocene. Radiocarbon 59, 395–405.

Lasher, G.E., Axford, Y., 2019. Medieval warmth confirmed at the Norse Eastern Settlement in Greenland. Geology 47 (3), 267–270.

Lenssen, N.J.L., Schmidt, G.A., Hansen, J.E., Menne, M.J., Persin, A., Ruedy, R., Zyss, D., 2019. Improvements in the GISTEMP uncertainty model. J. Geophys. Res. Atmos. 124 (12), 6307–6326.

Lewis, N., 2023. Objectively combining climate sensitivity evidence. Clim. Dyn. 60, 3139–3165.

Lindzen, R.S., Choi, Y.-S., 2011. On the observational determination of climate sensitivity and its implications. Asia-Pacific J. Atmos. Sci. 47, 377–390.

Ljungqvist, F.C., 2010. A new reconstruction of temperature variability in the extra-tropical northern hemisphere during the last two millennia. Geogr. Ann. Ser. A 92, 339–351.

Loehle, C., McCulloch, J.H., 2008. Correction to: A 2000-year global temperature reconstruction based on non-tree ring proxies. Energy Environ. 19 (1), 93–100.

Lüning, S., Gałka, M., Bamonte, F.P., Rodríguez, F.G., Vahrenholt, F., 2019. The Medieval Climate Anomaly in South America. Quat. Int. 508, 70–87.

Luterbacher, J., Werner, J.P., Smerdon, J.E., et al., 2016. European summer temperatures since Roman times. Environ. Res. Lett. 11, 024001.

Manabe, S., Wetherald, R., 1967. Thermal equilibrium of the atmosphere with a given distribution of relative humidity. J. Atmos. Sci. 24, 241–259.

Manabe, S., Wetherald, R., 1975. The effects of doubling the CO_2 concentration on the climate of a general circulation model. J. Atmos. Sci. 32, 3–15.

Mann, M.E., Zhang, Z., Hughes, M.K., Bradley, R.S., Miller, S.K., Rutherford, S., Ni, F., 2008. Proxy-based reconstructions of hemispheric and global surface temperature variations over the past two millennia. Proc. Natl. Acad. Sci. 105 (36), 13252–13257.

Masson-Delmotte, V., Zhai, P., Pörtner, H.-O., Roberts, D., Skea, J., Shukla, P., Pirani, A., Moufouma-Okia, W., Péan, C., Pidcock, R., Connors, S., Matthews, J., Chen, Y., X.Zhou, M.G., Lonnoy, E., Maycock, T., Tignor, M., , (eds.), T.W., 2018. IPCC, 2018: Global Warming of 1.5°C. An IPCC Special Report on the impacts of global warming of 1.5 °C above pre-industrial levels and related global greenhouse gas emission pathways, in the context of strengthening the global response to the threat of climate change, sustainable development, and efforts to eradicate poverty. Cambridge University Press.

Masson-Delmotte, V., Zhai, P., Pirani, A., Connors, S., Péan, C., Berger, S., Caud, N., Chen, Y., Goldfarb, L., Gomis, M., Huang, M., Leitzell, K., Lonnoy, E., Matthews, J., Maycock, T., Waterfield, T., Yelekci, O., Yu, R., (eds.), B.Z., 2021. IPCC, 2021: Climate Change 2021: The Physical Science Basis. Contribution of Working Group I to the Sixth Assessment Report of the Intergovernmental Panel on Climate Change. Cambridge University Press.

Matthes, K., Funke, B., Andersson, M.E., Barnard, L., Beer, J., Charbonneau, P., Clilverd, M.A., deWit, T.D., Haberreiter, M., Hendry, A., Jackman, C.H., Kretzschmar, M., Kruschke, T., Kunze, M., Langematz, U., Marsh, D.R., Maycock, A.C., Misios, S., Rodger, C.J., Scaife, A.A., Seppälä, A., Shangguan, M., Sinnhuber, M., Tourpali, K., Usoskin, I., vande Kamp, M., Verronen, P.T., Versick, S., 2017. Solar forcing for CMIP6 (v3.2). Geosci. Model Dev. 10, 2247–2302.

Mauritsen, T., Roeckner, E. (2020). Tuning the MPI-ESM1.2 global climate model to improve the match with instrumental record warming by lowering its climate sensitivity. Journal of Advances in Modeling Earth Systems, 12, e2019MS002037.

Mauritsen, T., Bader, J., Becker, T., Behrens, J., Bittner, M., Brokopf, R., et al., 2019. Developments in the MPI-M Earth System Model version 1.2 (MPI-ESM1.2) and its response to increasing CO2. J. Adv. Model. Earth Syst. 11, 998–1038.

McCarthy, G.D., Caesar, L., 2023. Can we trust projections of AMOC weakening based on climate models that cannot reproduce the past? Philosophical Transaction of the Royal Society A 381: 20220193.

McKitrick, R., Christy, J., 2020. Pervasive warming bias in CMIP6 tropospheric layers. Earth Space Sci. 7 (9).

McNutt, M., 2015. The beyond-two-degree inferno. Science 349, 7.

Mears, C.A., Wentz, F.J., 2016. Sensitivity of satellite-derived tropospheric temperature trends to the diurnal cycle adjustment. J. Clim. 29 (10), 3629–3646.

Meinshausen, M., Nicholls, Z.R.J., Lewis, J., Gidden, M.J., Vogel, E., Freund, M., Beyerle, U., Gessner, C., Nauels, A., Bauer, N., Canadell, J.G., Daniel, J.S., John, A., Krummel, P.B., Luderer, G., Meinshausen, N., Montzka, S.A., Rayner, P.J., Reimann, S., Smith, S.J., van den Berg, M., Velders, G.J.M., Vollmer, M.K., Wang, R.H.J., 2020. The shared socio-economic pathway (SSP) greenhouse gas concentrations and their extensions to 2500. Geosci. Model Dev. 13, 3571–3605.

Meinshausen, M., Lewis, J., McGlade, C., Gütschow, J., Nicholls, Z., Burdon, R., Cozzi, L., Hackmann, B., 2022. Realization of Paris Agreement pledges may limit warming just below 2 °C. Nature 604, 304–309.

Meinshausen, M., Schleussner, C.-F., Beyer, K., Bodeker, G., Boucher, O., Canadell, J. G., Daniel, J.S., Diongue-Niang, A., Driouech, F., Fischer, E., Forster, P., Grose, M., Hansen, G., Hausfather, Z., Ilyina, T., Kikstra, J.S., Kimutai, J., King, A., Lee, J.-Y., Lennard, C., Lissner, T., Nauels, A., Peters, G.P., Pirani, A., Plattner, G.-K., Pörtner, H., Rogelj, J., Rojas, M., Roy, J., Samset, B.H., Sanderson, B.M., Séférian, R., Seneviratne, S., Smith, C.J., Szopa, S., Thomas, A., Urge-Vorsatz, D., Velders, G.J. M., Yokohata, T., Ziehn, T., Nicholls, Z., 2023. A perspective on the next generation of Earth system model scenarios: towards representative emission pathways (REPs). Geosci. Model Dev. Discuss. [preprint]. https://doi.org/10.5194/gmd-2023-176. in review.

Mignot, J., Hourdin, F., Deshayes, J., Boucher, O., Gastineau, G., Musat, I., et al. (2021). The tuning strategy of IPSL-CM6A-LR. Journal of Advances in Modeling Earth Systems, 13, e2020MS002340.

Mitchell, D., Lo, Y.E., Seviour, W., Haimberger, L., Polvani, L., 2020. The vertical profile of recent tropical temperature trends: Persistent model biases in the context of internal variability. Environ. Res. Lett. 15 (10), 1040b4.

Moberg, A., Sonechkin, D., Holmgren, K., Datsenko, N.D., Karlén, W., 2005. Highly variable Northern Hemisphere temperatures reconstructed from low- and high-resolution proxy data. Nature 433, 613–617.

Möller, F., 1963. On the influence of changes in the CO_2 concentration in air on the radiation balance of the earth's surface and on the climate. J. Geophys. Res. 68, 3877–3886.

Monckton, C., Soon, W.-H., Legates, D.R., Briggs, W.M., 2015. Why models run hot: Results from an irreducibly simple model. Science Bulletin 60, 122–135.

Morice, C.P., Kennedy, J.J., Rayner, N.A., Winn, J.P., Hogan, E., Killick, R.E., Dunn, R. J. H., Osborn, T.J., Jones, P.D., Simpson, I.R., 2021. An updated assessment of near-surface temperature change from 1850: The HadCRUT5 data set. Journal of Geophysical Research: Atmospheres 126(3), e2019JD032361.

Morice, C.P., Kennedy, J.J., Rayner, N.A., Jones, P.D., 2012. Quantifying uncertainties in global and regional temperature change using an ensemble of observational estimates: The HadCRUT4 dataset. J. Geophys. Res. 117, D08101.

Neff, U., Burns, S.J., Mangini, A., Mudelsee, M., Fleitmann, D., Matter, A., 2001. Strong coherence between solar variability and the monsoon in Oman between 9 and 6 kyr ago. Nature 411, 290–293.

Nijsse, F.J.M.M., Cox, P.M., Williamson, M.S., 2020. Emergent constraints on transient climate response (TCR) and equilibrium climate sensitivity (ECS) from historical warming in CMIP5 and CMIP6 models. Earth Syst. Dyn. 11 (3), 737–750.

O'Neill, P., Connolly, R., Connolly, M., Soon, W., Chimani, B., Crok, M., de Vos, R., Harde, H., Kajaba, P., Nojarov, P., Przybylak, R., Rasol, D., Skrynyk, O., Skrynyk, O., Štěpánek, P., Wypych, A., Zahradníček, P., 2022. Evaluation of the Homogenization Adjustments Applied to European Temperature Records in the Global Historical Climatology Network Dataset. Atmos. 13, 285.
PAGES2k Consortium, 2017. A global multiproxy database for temperature reconstructions of the Common Era. Sci. Data 4, 170088.
Penza, V., Berrilli, F., Bertello, L., Cantoresi, M., Criscuoli, S., Giobbi, P., 2022. Total solar irradiance during the last five centuries. Astrophys. J. 937 (2), 84.
Piao, S., Wang, X., Park, T., Chen, C., Lian, X., He, Y., Bjerke, J.W., Chen, A., Ciais, P., Tømmervik, H., Nemani, R.R., Myneni, R.B., 2019. Characteristics, drivers and feedbacks of global greening. Nature Reviews Earth & Environment 1 (1), 14–27.
Pielke, R., Burgess, M.G., Ritchie, J., 2022. Plausible 2005–2050 emissions scenarios project between 2 °C and 3 °C of warming by 2100. Environ. Res. Lett. 17, 024027.
Pielke, R., Ritchie, J., 2021a. Distorting the view of our climate future: The misuse and abuse of climate pathways and scenarios. Energy Res. Soc. Sci. 72, 101890.
Pielke, R., Ritchie, J., 2021b. How climate scenarios lost touch with reality. Issues Sci. Technol. 37 (4), 75–83.
Pielke, R., 2021. How to Understand the New IPCC Report: Part 1, Scenarios. The Honest Broker. https://rogerpielkejr.substack.com/p/how-to-understand-the-new-ipcc-report.
Pörtner, H.-O., Roberts, D., Tignor, M., Poloczanska, E., Mintenbeck, K., Alegría, A., Craig, M., Langsdorf, S., Löschke, S., Möller, V., Okem, A., (eds.), B.R., 2022. IPCC, 2022: Climate Change 2022: Impacts, Adaptation and Vulnerability. Contribution of Working Group II to the Sixth Assessment Report of the Intergovernmental Panel on Climate Change. Cambridge University Press.
Rahmstorf, S., 2008. Anthropogenic climate change: Revisiting the facts. In: Zedillo, E. (Ed.), Global Warming: Looking Beyond Kyoto. Brookings Institution Press, Washington, Ch.3, pp. 34–53.
Riahi, K., van Vuuren, D.P., Kriegler, E., Edmonds, J., O'Neill, B.C., Fujimori, S., Bauer, N., Calvin, K., Dellink, R., Fricko, O., Lutz, W., Popp, A., Cuaresma, J.C., Leimbach, M., Jiang, L., Kram, T., Rao, S., Emmerling, J., Ebi, K., Hasegawa, T., Havlik, P., Humpenöder, F., Silva, L.A.D., Smith, S., Stehfest, E., Bosetti, V., Eom, J., Gernaat, D., Masui, T., Rogelj, J., Strefler, J., Drouet, L., Krey, V., Luderer, G., Harmsen, M., Takahashi, K., Baumstark, L., Doelman, J.C., Kainuma, M., Klimont, Z., Marangoni, G., Lotze-Campen, H., Obersteiner, M., Tabeau, A., Tavoni, M., 2017. The shared socioeconomic pathways and their energy, land use, and greenhouse gas emissions implications: An overview. Glob. Environ. Chang. 42, 153–168.
Ritchie, J., Dowlatabadi, H., 2017. Why do climate change scenarios return to coal? Energy 140 (P1), 1276–1291.
Rocque, R.J., Beaudoin, C., Ndjaboue, R., Cameron, L., Poirier-Bergeron, L., Poulin-Rheault, R.-A., Fallon, C., Tricco, A.C., Witteman, H.O., 2021. Health effects of climate change: an overview of systematic reviews. BMJ Open 11 (6), e046333.
Roe, G., 2009. Feedbacks, timescales, and seeing red. Annu. Rev. Earth Planet. Sci. 37 (1), 93–115.
Rohde, R.A., Hausfather, Z., 2020. The Berkeley earth land/ocean temperature record. Earth Syst. Sci. Data 12 (4), 3469–3479.
Rugenstein, M., Zelinka, M., Karnauskas, K.B., Ceppi, P., Andrews, T., 2023. Patterns of surface warming matter for climate sensitivity. EOS 104. https://doi.org/10.1029/2023EO230411.
Santer, B., Fyfe, J., Pallotta, G., Pallotta, G., Flato, G.M., Meehl, G.A., England, M.H., Hawkins, E., Mann, M.E., Painter, J.F., Bonfils, C., Cvijanovic, I., Mears, C., Wentz, F.J., Po-Chedley, S., Fu, Q., Zou, C.-Z., 2017. Causes of differences in model and satellite tropospheric warming rates. Nature Geoscience 10, 478–485.
Scafetta, N., 2010. Empirical evidence for a celestial origin of the climate oscillations and its implications. J. Atmos. Sol. Terr. Phys. 72, 951–970.
Scafetta, N., 2012a. Testing an astronomically based decadal-scale empirical harmonic climate model versus the IPCC (2007) general circulation climate models. J. Atmos. Sol. Terr. Phys. 80, 124–137.
Scafetta, N., 2012b. Multi-scale harmonic model for solar and climate cyclical variation throughout the Holocene based on Jupiter-Saturn tidal frequencies plus the 11-year solar dynamo cycle. J. Atmos. Sol. Terr. Phys. 80, 296–311.
Scafetta, N., 2013. Discussion on climate oscillations: CMIP5 general circulation models versus a semi-empirical harmonic model based on astronomical cycles. Earth Sci. Rev. 126, 321–357.
Scafetta, N., 2014a. Multi-scale dynamical analysis (MSDA) of sea level records versus PDO, AMO, and NAO indexes. Clim. Dyn. 43, 175–192.
Scafetta, N., 2014b. Discussion on the spectral coherence between planetary, solar and climate oscillations: a reply to some critiques. Astrophys. Space Sci. 354, 275–299.
Scafetta, N., 2020. Solar Oscillations and the Orbital Invariant Inequalities of the Solar System. Sol. Phys. 295 (2), 33.
Scafetta, N., 2021a. Detection of non-climatic biases in land surface temperature records by comparing climatic data and their model simulations. Clim. Dyn. 56 (9–10), 2959–2982.
Scafetta, N., 2021b. Reconstruction of the interannual to millennial scale patterns of the global surface temperature. Atmos. 12 (2), 147.
Scafetta, N., 2021c. Testing the CMIP6 GCM simulations versus surface temperature records from 1980–1990 to 2011–2021: High ECS is not supported. Climate 9 (11), 161.
Scafetta, N., 2023a. CMIP6 GCM ensemble members versus global surface temperatures. Clim. Dyn. 60, 3091–3120.
Scafetta, N., 2023b. CMIP6 GCM validation based on ECS and TCR ranking for 21st century temperature projections and risk assessment. Atmos. 14 (2), 345.
Scafetta, N., 2023c. Empirical assessment of the role of the sun in climate change using balanced multi-proxy solar records. Geosci. Front. 14, (6) 101650.
Scafetta, N., Bianchini, A., 2023. Overview of the spectral coherence between planetary resonances and solar and climate oscillations. Climate 11 (4), 77.
Scafetta, N., Milani, F., Bianchini, A., 2020. A 60-Year cycle in the meteorite fall frequency suggests a possible interplanetary dust forcing of the Earth's climate driven by planetary oscillations. Geophysical Research Letters 47(18), e2020GL089954.
Scafetta, N., Ouyang, S., 2019. Detection of UHI bias in China climate network using Tmin and Tmax surface temperature divergence. Global Planet. Change 181, 102989.
Scafetta, N., Humlum, O., Solheim, J.-E., Stordahl, K., 2013. Comment on "The influence of planetary attractions on the solar tachocline" by Callebaut, de Jager and Duhau. J. Atmos. Sol. Terr. Phys. 102, 368–371.
Scafetta, N., Milani, F., Bianchini, A., Ortolani, S., 2016. On the astronomical origin of the Hallstatt oscillation found in radiocarbon and climate records throughout the Holocene. Earth Sci. Rev. 162, 24–43.
Scafetta, N., Willson, R., Lee, J., Wu, D., 2019. Modeling quiet solar luminosity variability from TSI satellite measurements and proxy models during 1980–2018. Remote Sens. (Basel) 11, 2569.
Scafetta, N., 2022. Advanced testing of low, medium, and high ECS CMIP6 GCM simulations versus ERA5-T2m. Geophysical Research Letters 49(6), e2022GL097716.
Scafetta, N., 2023d. Reply to "Comment on 'Advanced testing of low, medium, and high ECS CMIP6 GCM simulations versus ERA5-T2m' by N. Scafetta (2022)" by Schmidt et al. (2023). Geophysical Research Letters, 50, e2023GL104960.
Schmidt, G.A., Jones, G.S., Kennedy, J.J., 2023. Comment on "Advanced testing of low, medium, and high ECS CMIP6 GCM simulations versus ERA5-T2m" by N. Scafetta (2022). Geophysical Research Letters 50, e2022GL102530.
Schmutz, W.K., 2021. Changes in the total solar irradiance and climatic effects. J. Space Weather Space Clim. 11, 40.
Shaviv, N.J., 2002. Cosmic ray diffusion from the galactic spiral arms, iron meteorites, and a possible climatic connection. Phys. Rev. Lett. 89, (5) 051102.
Sherwood, S., Webb, M., Annan, J., Armour, K., Forster, P., Hargreaves, J., Hegerl, G., Klein, S., Marvel, K., Rohling, E., Watanabe, M., Andrews, T., Braconnot, P., Bretherton, C., Foster, G., Hausfather, Z., von der Heydt, A., Knutti, R., Mauritsen, T., Norris, J., Proistosescu, C., Rugenstein, M., Schmidt, G., Tokarska, K., Zelinka, M., 2020. An assessment of earth's climate sensitivity using multiple lines of evidence. Reviews of Geophysics 58, e2019RG000678.
Shukla, P., Skea, J., Reisinger, A., Slade, R., Fradera, R., Pathak, M., Khourdajie, A., Belkacemi, M., van Diemen, R., Hasija, A., Lisboa, G., Luz, S., Malley, J., McCollum, D., Some, S., (eds.), P.V., 2022. IPCC, 2022: Climate Change 2022: Mitigation of Climate Change. Contribution of Working Group III to the Sixth Assessment Report of the Intergovernmental Panel on Climate Change. Cambridge University Press.
Soon, W., Connolly, R., Connolly, M., Akasofu, S.-I., Baliunas, S., Berglund, J., Bianchini, A., Briggs, W.M., Butler, C.J., Cionco, R.G., et al., 2023. The Detection and Attribution of Northern Hemisphere Land Surface Warming (1850–2018) in Terms of Human and Natural Factors: Challenges of Inadequate Data. Climate 11, 179.
Spencer, R.W., Christy, J.R., 2023. Effective climate sensitivity distributions from a 1D model of global ocean and land temperature trends, 1970–2021. Theor. Appl. Climatol. https://doi.org/10.1007/s00704-023-04634-7.
Spencer, R.W., Christy, J.R., Braswell, W.D., 2017. UAH version 6 global satellite temperature products: Methodology and results. Asia-Pac. J. Atmos. Sci. 53 (1), 121–130.
Spencer, R.W., 2023. Examples from our New UAH Urban Heat Island Dataset. https://www.drroyspencer.com/2023/11/examples-from-our-new-uah-urban-heat-island-dataset/. (access December 7 2023).
Stefani, F., 2021. Solar and Anthropogenic Influences on Climate: Regression Analysis and Tentative Predictions. Climate 9, 163.
Steinhilber, F., Abreu, J.A., Beer, J., Brunner, I., Christl, M., Fischer, H., Heikkilä, U., Kubik, P.W., Mann, M., McCracken, K.G., Miller, H., Miyahara, H., Oerter, H., Wilhelms, F., 2012. 9,400 years of cosmic radiation and solar activity from ice cores and tree rings. Proc. Natl. Acad. Sci. 109 (16), 5967–5971.
Stocker, T.F., D. Qin, G.-K. Plattner, M. Tignor, S.K. Allen, J. Boschung, A. Nauels, Y. Xia, V. Bex and P.M. Midgley (eds.). IPCC, 2013: Climate Change 2013: The Physical Science Basis. Contribution of Working Group I to the Fifth Assessment Report of the Intergovernmental Panel on Climate Change. Cambridge University Press, Cambridge, United Kingdom and New York, NY, USA.
Svensmark, J., Enghoff, M.B., Shaviv, N.J., Svensmark, H., 2016. The response of clouds and aerosols to cosmic ray decreases. J. Geophys. Res. Space Phys. 121 (9), 8152–8181.
Svensmark, H., 2022. Supernova rates and burial of organic matter. Geophysical Research Letters 49(1), e2021GL096376.
Tol, R.S.J., 2015. Who benefits and who loses from climate change? In: Handbook of Climate Change Mitigation and Adaptation. Springer, New York, pp. 1–12.
UNFCCC, 2023. The Paris Agreement: What is the Paris Agreement? https://unfccc.int/process-and-meetings/the-paris-agreement. (access 10 June 2023).
van Oldenborgh, G., 2020. The knmi climate explorer: Knmi (results, code)/world meteorological organization (wmo) (design). https://climexp.knmi.nl/start.cgi.
Tol, R., 2023. Costs and benefits of the Paris climate targets. Climate Change Economics 14, 2340003.
van Vuuren, D.P., Edmonds, J., Kainuma, M., Riahi, K., Thomson, A., Hibbard, K., Hurtt, G.C., Kram, T., Krey, V., Lamarque, J.-F., Masui, T., Meinshausen, M.,

Nakicenovic, Smith, S.J., Rose, S.K., 2023. The representative concentration pathways: an overview. Clim. Change 109, 5–31.
Voosen, P., 2019. New climate models forecast a warming surge. Science 364, 222–223.
Voosen, P., 2021. Climate panel confronts implausibly hot models. Science 373, 474–475.
Wu, C.-J., Krivova, N.A., Solanki, S.K., Usoskin, I.G., 2018. Solar total and spectral irradiance reconstruction over the last 9000 years. A & A 620, A120.
Wyatt, M.G., Curry, J.A., 2013. Role for Eurasian arctic shelf sea ice in a secularly varying hemispheric climate signal during the 20th century. Clim. Dyn. 42 (9–10), 2763–2782.
Zhang, H.-M., Lawrimore, J., Huang, B., Menne, M., Yin, X., Sánchez-Lugo, A., Gleason, B., Vose, R., Arndt, D., Rennie, J., Williams, C. Updated temperature data give a sharper view of climate trends, Eos, 100. EOS 100. https://doi.org/10.1029/2019EO128229.
Zhu, Z., Piao, S., Myneni, R.B., Huang, M., Zeng, Z., Canadell, J.G., Ciais, P., Sitch, S., Friedlingstein, P., Arneth, A., Cao, C., Cheng, L., Kato, E., Koven, C., Li, Y., Lian, X., Liu, Y., Liu, R., Mao, J., Pan, Y., Peng, S., Peñuelas, J., Poulter, B., Pugh, T.A.M., Stocker, B.D., Viovy, N., Wang, X., Wang, Y., Xiao, Z., Yang, H., Zaehle, S., Zeng, N., 2016. Greening of the earth and its drivers. Nat. Clim. Chang. 6 (8), 791–795.
Zou, C.-Z., Xu, H., Hao, X., Liu, Q., 2023. Mid-tropospheric layer temperature record derived from satellite microwave sounder observations with backward merging approach. Journal of Geophysical Research: Atmospheres 128, e2022JD037472.